Turkish Journal of Earth Sciences (Turkish J. Earth Sci.), Vol. 18, 2009, pp. 139–162. *Copyright ©TÜBİTAK*
doi:10.3906/yer-0806-7 First published online 07 July 2008

Alteration Mineralogy and Geochemistry of the Hydrothermally Altered Rocks of the Kutlular (Sürmene) Massive Sulfide Deposit, NE Turkey

EMEL ABDİOĞLU & MEHMET ARSLAN

Department of Geological Engineering, Karadeniz Technical University,TR–61080 Trabzon, Turkey

(E–mail: abdioglu@ktu.edu.tr)

Received 01 April 2007; revised typescript received 06 December 2007; accepted 13 February 2008

Abstract: Volcanogenic massive sulfide deposits accompanying the Upper Cretaceous felsic rocks in the intra-arc rift zone of the Pontide palaeo-arc are common in the NE Turkey. One of them, the Kutlular (Sürmene, Trabzon) deposit, is an abandoned mine within the Upper Cretaceous mafic, felsic volcanics and subvolcanic rocks.

Detailed mineralogical and geochemical studies indicate the presence of hydrothermal alteration zones around the Kutlular deposit; these alteration zones are represented by silicification-pyrite-illite zone, illite-silicification zone, illite/smectite-silicification zone, smectite zone accompanying kaolinite and halloysite in the dacitic pyroclastics, and additionally chlorite zone in the mafic volcanics. Lithogeochemical data indicate that the footwall dacitic rocks (Zr/Y= 1.39–16.39, La/Yb= 0.14–9.57) and hanging-wall basalts-basaltic andesites (Zr/Y= 2.13–5.65, La/Yb= 1.16–5.00) are transitional between tholeiitic and calc-alkaline in character. The trace element patterns of the rocks show considerable LILE enrichment (K, Rb and Ba) and depletion in Sr and Ti relative to N-type MORB. Chondrite-normalized REE patterns of the footwall show pronounced HREE enrichment. The Kutlular footwall and hanging wall alteration zones have several geochemical characteristics that show systematic changes with increasing proximity to ore body such as Na depletion as well as elevated alteration index (AI) and chlorite-carbonate-pyrite index (CCPI). Generally, hanging-wall mafic volcanics and footwall rocks have high CCPI (chlorite-carbonate-pyrite index) values, indicating the importance of chlorite and pyrite formation in these rocks. Calculated mass changes in the footwall dacites commonly are large, and result from major silica mass transfer (–9.11 to 99.68 g/100 g rock). Mass-change calculations indicate that CaO + Na_2O + MgO were leached from the rocks by hydrothermal solutions, whereas large amounts of hydrothermal iron were added. Hanging wall basalt and basaltic andesite shows mass changes that are generally much smaller than in the footwall.

Key Words: hydrothermal alteration, clay minerals, massive sulfide deposit, eastern Pontides, Turkey

Kutlular (Sürmene, Trabzon) Masif Sülfit Yatağı Çevresindeki Hidrotermal Altere Kayaçların Alterasyon Mineralojisi ve Jeokimyaları, KD Türkiye

Özet: Eski bir adayayı kalıntısı olan Pontidler'de yay içi rift zonunda oluşan Geç Kretase yaşlı felsik kayaçlar volkanojenik masif sülfit yataklarına ev sahipliği yaparlar. Bunların arasında, terkedilmiş bir maden olan Kutlular masif sülfit yatağı (Sürmene, Trabzon) Geç Kretase yaşlı mafik, felsik ve subvolkanik kayaçları içerir.

Ayrıntılı mineralojik ve jeokimyasal çalışmalar Kutlular yatağı çevresinde hidrotermal alterasyon zonlarının varlığını göstermiştir. Bu zonlar; dasitik piroklastitlerde silisleşme-pirit-illit zonu, illit-silisleşme zonu, illit/simektit-silisleşme zonu, simektit zonu ve buna eşlik eden kaolenit ve halloysit ile temsil edilirken, mafik volkanitlerde klorit zonu iyi gelişmiştir. Litokimyasal veriler ışığında cevherli dasitik kayaçlar (Zr/Y= 1.39–16.39, La/Yb= 0.14–9.57) ve örtü kayaçları olan bazaltik-andezitik kayaçlar (Zr/Y= 2.13–5.65, La/Yb= 1.16–5.00) toleyitik-kalkalkalen karakterlidir. Tüketilmiş okyanus ortası sırtı bazaltına (N-MORB) normalize iz element değişimlerine göre örnekler büyük iyon yarıçaplı litofil elementler (LILE; K, Rb ve Ba) bakımından zenginleşmiş, Sr ve Ti bakımından ise tüketilmişlerdir. Cevherin içerisinde bulunduğu dasitik kayaçların kondrite normalize nadir toprak element (REE) değişimleri ağır nadir toprak elementler (HREE) bakımından zenginleşme göstermektedir. Kutlular madeni taban ve örtü kayaçları alterasyon zonları cevhere yaklaştıkça sistematik olarak Na'ca tüketilme, alterasyon indeksi (AI) ve klorit-karbonat-pirit indeksinde (CCPI) artışlarla ifade edilebilecek jeokimyasal karakteristikler sergilerler. CCPI değeri örtü kayaçları konumundaki mafik volkanitler ve cevherin içerisinde bulunduğu felsik kayaçlarda kloritleşme ve pirit oluşumunun önemini ifade eder şekilde yüksektir. Cevherli dasitlerde hesaplanan kütle değişimi oldukça büyüktür ve genelde SiO_2'deki değişimlerden kaynaklanır (–9.11 to 99.68 gr/100 gr kayaç). Kütle değişim hesaplarına göre CaO + Na_2O + MgO hidrotermal akışkanlarca kayaçlardan yıkanmış; buna karşın büyük miktarda demir eklenmiştir. Örtü kayaçları bazalt ve bazaltik andezitler kütle değişiminden daha az oranda etkilenmişlerdir.

Anahtar Sözcükler: hidrotermal alterasyon, kil mineralleri, masif sülfit yatağı, Doğu Pontidler, Türkiye

Introduction

Volcanogenic massive Cu-Zn-(Pb) sulfide (VMS) deposits develop primarily in subaqueous rift-related environments (e.g., oceanic, fore-arc, arc, back-arc, continental margin, or continental), and are hosted primarily by bimodal, mafic-felsic volcanic successions, with specific geochemical characteristics (e.g., Hart *et al.* 2004). The eastern Pontide volcanic province is part of the Tethyan-Eurasia

metallogenic belt, which extends from east Europe to middle Asia-Pacific and hosts economically important ore deposits (Pejatoviç 1979). The zone, located in the eastern Black Sea region extending E–W along 350 km and N–S along 60 km, is described Pontide metallogenic belt (Akıncı 1980). In the region, VMS deposits accompanying the Upper Cretaceous felsic volcanics are common (Çağatay & Boyle 1977; Leitch 1981; Schneider *et al.* 1988; Çağatay 1993; Tüysüz 2000; Akçay 2008) and potentially important in the Cu, Pb and Zn productions. These deposits have features similar to the Kuroko-type deposits in Japan and commonly occur within intensely altered felsic volcanic rocks (Sato 1977; Leitch 1981; Urabe & Marumo 1991; Çağatay 1993; Antonović *et al.* 1996; Barrett & MacLean 1999; Akçay & Moon 2001; Akçay 2008). The abandoned Kutlular mine (Sürmene, Trabzon), one of the largest volcanogenic massive sulfide (VMS) deposit in Turkey, is located about 4 km south of the Black Sea coastline and 14 km to the east of Sürmene (Trabzon) in NE Turkey (Figure 1).

The mineralogy and lithogeochemistry of the hydrothermally altered volcanic rocks have been extensively used to define hydrothermal alteration haloes. Many attempts have been made to define mineralogy, chemistry and chemical changes of hydrothermally altered footwall and hanging wall in several VMS deposits around the world (e.g., Bryndzia *et al.* 1983; Urabe *et al.* 1983; MacLean & Kranidiotis 1987; Barriga & Fyfe 1988; Large 1992; Barret *et al.* 1993a, b; Çağatay 1993; Çağatay & Eastoe 1995; Barret *et al.* 1996; Lentz & Goodfellow 1996; Ohmoto 1996; Peter & Goodfellow 1996; Almodóvar *et al.* 1998; Leistel *et al.* 1998; Gibson *et al.* 1999; Paulick & McPhie 1999; Sánchez-España *et al.* 2000; Paulick *et al.* 2001; Akçay 2003, 2008). This paper presents the results of mineralogical and geochemical studies of hydrothermal alteration zones associated with the Kutlular massive sulfide deposit in NE Turkey.

Geological Setting

The eastern Pontides, located along the Alpine metallogenic belt, is one of the best-preserved examples of a palaeo-arc setting formed by subduction of the Tethyan ocean crust from Jurassic to Miocene (Dixon & Pereira 1974; Şengör & Yılmaz 1981; Okay & Şahintürk 1997). Although many authors are still disputing about the polarity and timing of the subduction and formation of the eastern Pontides (Şengör & Yılmaz 1981; Bektaş 1987; Bektaş *et al.* 1998; Boztuğ *et al.* 2004, 2006, 2007), it is known that subduction was completed by middle Eocene (Adamia *et al.* 1981; Okay & Şahintürk 1997). The eastern Pontides straddle the North Anatolian transform fault and display three major volcanic cycles of Liassic, Late Cretaceous and Tertiary age. Volcanic rocks of Liassic age are transitional, those of Late Cretaceous ages are subalkaline, and Eocene volcanic rocks are alkaline and subalkaline in character (Arslan *et al.* 1997, 2007; Arslan & Aslan 2006). Volcanism in the region began during the Liassic time with the formation of basic rocks in a rift environment (Tokel 1972; Schneider *et al.* 1988; Arslan *et al.* 1997), developed on a Precambrian to Palaeozoic basement (Yılmaz 1972; Okay & Şahintürk 1997; Topuz *et al.* 2001; Topuz 2002). Liassic volcanism comprises of calcalkaline volcanic and volcanoclastics with locally deposited sedimentary rocks (Arslan *et al.* 1997). These units are overlain by Dogger to Lower Cretaceous platform carbonates. After the deposition of the carbonate rocks, island arc volcanic activity began (Eğin *et al.* 1979). In the Late Cretaceous, early mafic rocks were followed by felsic rock series, and then by upper mafic rocks. These rocks are composed of dacites and basalts with calc-alkaline composition, and reflect the features of the arc volcanism (Tokel 1977). The Upper Cretaceous rocks host the volcanogenic massive sulphide (VMS) deposits in the region. The Kutlular and other VMS deposits (e.g., Murgul, Lahanos and Çayeli) are located in the intra-arc rift zone of the Pontide island arc.

Material and Methods

Eighty samples of mafic and felsic rocks of the Kutlular area were selected for optical microscope, X-ray diffraction and lithogeochemical studies. Optical microscope studies were carried out on lavas, pyroclastics and partly altered rocks. Selected samples for geochemical and X-ray diffraction (XRD) analyses were ground using an agate mortar and pestle. In order to obtain clay fractions (<2 μm), chemical treatments (Jackson 1956; Mehra & Jackson 1960; Kunze 1965) were carried out to remove carbonates, amorphous silica and free Fe oxides. After that, clay fractions (<2 μm) were separated by sedimentation, followed by centrifugation of the suspension after overnight dispersion in distilled water. More complete dispersion of clay particles was achieved by ultrasonic treatment for

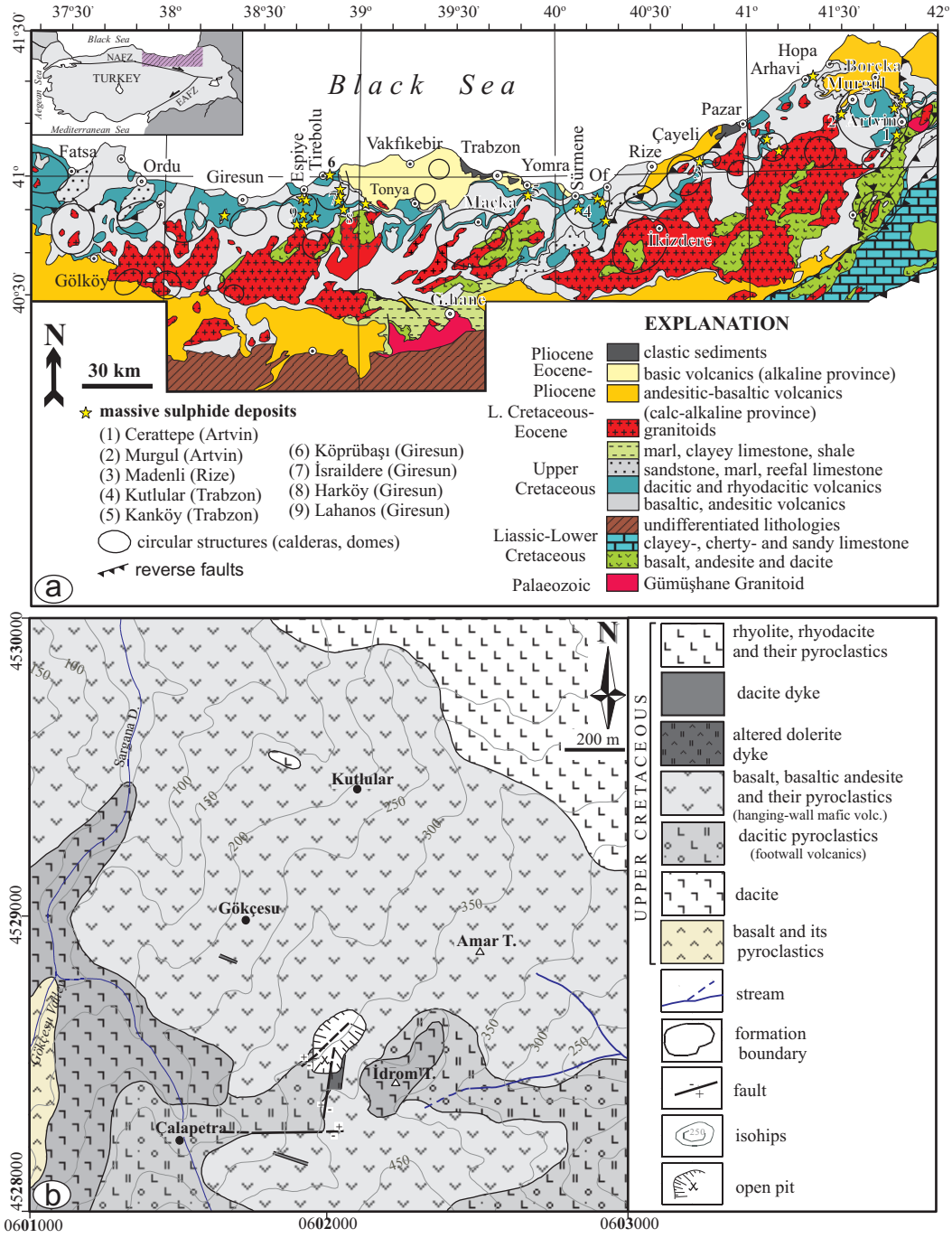

Figure 1. (a) The simplified geological map of the eastern Pontides. The Kutlular and the other significant massive sulfide deposits are marked on the map (simplified from Güven 1993 and Akçay & Moon 2001). (b) Geological map of the Kutlular (Sürmene-Trabzon) area in NE Turkey. NAFZ– North Anatolian Fault zone; EAFZ– East Anatolian Fault Zone.

~15 min. XRD analyses were carried out using a Rigaku DMAX 2200 and a Rigaku DMAXIIC X-ray diffractometre (Cu-Ka and Ni filter). Semi-quantitative mineral abundances were identified using the mineral intensity factors according to an external standard method (Brindley 1980). Oriented clay fractions were analyzed in the untreated state (N), after ethylene glycolation (EG; 60 °C, 16 h) and after heating (H; 300 and 550 °C).

Whole rock and clay fraction samples were analyzed for major, trace and rare earth element (REE) analysis. Chemical analyses of whole-rock and clay fractions were carried out by ICP-AES and ICP-MS at ACME Analytical Laboratories Ltd. (Canada). Detection limits range from 0.01 to 0.1 wt% for major elements, 0.1 to 5 ppm for trace elements and 0.01 to 0.5 ppm for the REE.

Results

Local Geology and Petrography

In the Kutlular area, Upper Cretaceous mafic, felsic volcanics and subvolcanic rocks crop out. The oldest rocks of the study area are formed by basalt and its pyroclastic derivatives. This unit is overlain by barren dacite and footwall dacite, respectively. The basalt, basaltic andesite and their pyroclastics as hanging-wall mafic rocks overly the footwall rocks. The altered dolerite and dacite dykes cut all the units.

The Kutlular massive sulphide deposit has generally massive, stringer and disseminated ore. It consists of three primary seafloor mineral assemblages and a supergene assemblage. The first primary association (black ore) includes mainly sphalerite, pyrite, galena, and tetrahedrite-tennantite. The second association (yellow ore) contains mainly of chalcopyrite, pyrite and lesser sphalerite and tetrahedrite-tennantite. The last one, pyritic ore, comprises pyrite, rare chalcopyrite and tetrahedrite-tennantite. The supergene mineralization consists of mainly covellite, chalcocite, bornite, malachite and azurite. The Kutlular mine has 1.26 Mt ore, 0.76 Mt (with an average grade of 2.4% Cu, 1.5% Zn and 0.04% Pb) of which was mined between 1986 and August 1992 (Çağatay & Eastoe 1995). According to Yıldız (1988), the weighted average content of Cu was 2.83 %. The massive sulfide lens was underlain mainly by dacitic tuff and covered by dacitic-pumiceous tuffs, dacitic breccias and basalt-basaltic andesite lavas that intruded by altered dolerite dyke. Before the mining activities, fine-grained gypsum occurrences could be observed as small pockets in the hanging wall pyroclastic rocks (Çağatay & Eastoe 1995).

Lower Units. Here the mafic volcanics, consisting of altered basalt and pyroclastics of similar composition, make up the basement rocks of the area. These rocks are well exposed along Gökçesu valley. The basaltic rocks are dark grey and blackish in colour and show microlitic porphyritic texture. The plagioclase is the main constituent of the rock. The groundmass consists mainly of plagioclase microlites, chlorite and opaque phases. The rocks are highly altered and secondary pyrite and lesser amount of chlorite, quartz, zeolite and clay minerals are also observed.

The lower dacites, mainly the dacites and to lesser extent dacitic pyroclastics are exposed along Gökçesu valley and İdrom Tepe. These rocks overlie the basement rocks and underlie the footwall dacitic rocks. Grey, greenish grey and white coloured barren dacite includes large quartz and feldspar crystals up to 3 mm as well as disseminated pyrite. The dacite exhibits porphyritic texture and contains quartz and plagioclase phenocrysts. Highly chloritized biotite pheno- and micro-crystals and disseminated opaques are also observed. The groundmass is formed by secondary quartz, albite, sericite, chlorite and clay minerals.

Footwall Rocks. The footwall rocks are variably hydrothermally altered and the intensity of alteration increases with proximity to the massive sulfide body. The footwall dacite is generally in the form of pyroclastics with only minor lavas, and is usually hydrothermally altered and surficially weathered. The volcanic breccias have angular to rounded pyroclasts, typically 7–20 cm. The pyroclasts are commonly vesicular and cemented with ash. In hand specimen, the broken surfaces of the dacitic rocks are beige, greyish white and altered surface is grey, light yellow, light brown and creamy white in colour. The intensity of surficial weathering and hydrothermal alteration affects the macroscopic view of the footwall dacite; the highly clayey-altered part of the rocks is very soft and whitish in colour while silicified parts are very hard and include visible disseminated pyrite of variable size.

Dacitic tuffs are characterized by abundant quartz pheno- and micro-crystal fragments in variable size, feldspar, altered pumice, dacitic lithic fragments, and

abundant amount of opaques, in a fine-grained matrix with Fe-oxide pigmentation (Figure 2a, b, e). Feldspar micro- and pheno-crystal fragments are partly silicified, argillizated and transformed into kaolinite and quartz (Figure 2d). Sericite occurs as replacement of plagioclase, mica and other aluminosilicate minerals, and as replacement of the groundmass, especially volcanic glass (Figure 2a, b). A quartz-sericite-pyrite mineral assemblage occurs mainly in the footwall rocks of the ore lens, as an inner alteration zone enveloping a core zone of silicification in the footwall. Chlorite, quartz, sericite and vitric fragments are other constituents of the rocks (Figure 2c–f). Pyrite is always present as disseminations (Figure 2f) and, to a lesser extent, as discontinuous veinlets within these rocks. Vuggy quartz is characterized by fine-grained quartz with abundant open spaces that are partly filled by clays and rarely other alteration minerals. Vugs typically are formed by dissolution of phenocrysts and vitric fragments of the pyroclastics in the dacitic rocks and are lined by quartz and pyrite. In many cases, the sulfides are oxidized, resulting in extensive limonite coatings around vugs. Quartz forms a dense mosaic texture.

The dacites generally show porphyritic and glassy textures. They contain euhedral and subhedral quartz microcrysts and phenocrysts. Plagioclase microlites and phenocrysts are partly silicified and sericitized. The groundmass includes secondary quartz, albite, chlorite and clay minerals. Skeletal ferromagnesian minerals are intensely fractured and occasionally chloritized and silicified. Open spaces such as vesicles, vugs and fractures are filled with chlorite.

Hanging-Wall Mafic Volcanics. In the studied area, hanging-wall mafic volcanics are well exposed above the footwall rocks and are composed mainly of basalt, basaltic andesite and their pyroclastic equivalents. They are best seen in the open pit area and surroundings. Their colour ranges from black to dark grey and locally reddish and yellowish black. Basalt and basaltic andesites exhibit physical weathering such as exfoliation but generally have well-developed columnar jointing. The unit locally shows silicification, chloritization, epidotization, argillization and is cut by quartz and calcite veinlets. The lower part of the lavas consists of ellipsoidal-circular shaped volatile spaces, whose diameter changes from 0.5 to 3 cm, partly embedded by quartz (in symmetrical), calcite and zeolite (e.g., laumontite, stilbite and analcime) infillings.

Basalt and basaltic andesite samples exhibit fluidal, microlitic, porphyritic, and vesicular and rarely aphanitic textures. Plagioclase (especially oligoclase and andesine) is the main rock-forming mineral, sometimes arranged sub-parallel to flow direction of lavas and found as both microlite and euhedral or subhedral phenocrysts. In some samples, plagioclase has been partly replaced by albite, calcite and zeolite (e.g., heulandite and laumontite). Albitization and carbonitization of primary plagioclase also occurs as reaction rims or along crystal fractures (Figure 3a–c). Minor amounts of epidote are generally found as infilling, surrounded by zeolite and calcite and sometimes as the patchy replacement of plagioclase (Figure 3b). Skeletal augite and olivine are rarely seen and may be intensely fractured, occasionally chloritized and lined by opaque rims (Figure 3d). Subhedral and euhedral opaque grains are always present. The groundmass is commonly altered to calcite and zeolite or partially to chlorite and clay minerals (smectite and illite). Chlorites are determined as infillings and replacement of glass in groundmass and glassy inclusions on sieve textured plagioclase (Figure 3c, d). The degree of alteration increases with fracture intensity, the presence of glassy matrix and distance to the massive ore lens.

Altered Dolerite Dyke. It is exposed in the Kutlular open pit area, northeast and south of the ore lens. Its colour changes from yellowish black to dark yellowish grey and plagioclase phenocrysts are described in naked eye and exhibit well-developed columnar jointing.

The altered dolerite dyke shows intersertal, poikilitic and ophitic textures. Plagioclases (labradorite) are the main constituents of the rock and are partly albitized, chloritized and sericitized. The angular interstices between plagioclase grains are occupied by grains of augite and pigeonite. Secondary minerals are represented by chlorite and calcite as vesicle infillings and alteration products of the primary minerals. Opaque minerals are seen in the micro-vesicles and voids of the rock.

Clay Mineralogy and Chemistry

Clay mineralogy of altered volcanic rocks was identified in detail by XRD studies. It should be pointed out here that the roentgenographically determined illite corresponds to optically determined sericite in these types of rocks (e.g., Środoń & Eberl 1984). Lower dacites include smectite, illite, kaolinite, and interstratified smectite/chlorite in

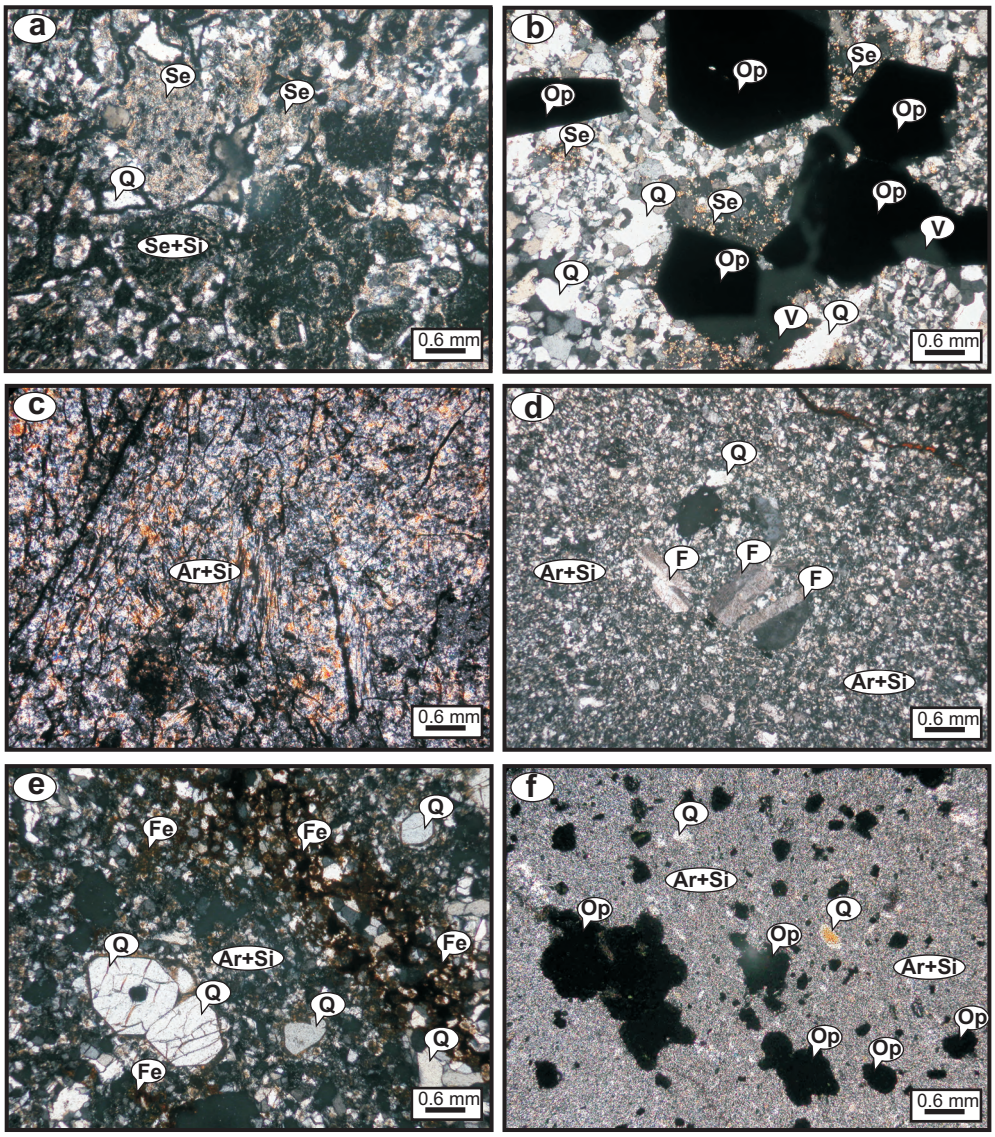

Figure 2. Photomicrographs of footwall dacites under crossed polars: **(a)** and **(b)** sericitization and silicification of volcanic glass in dacitic vitric-crystal tuff. Glass shards are replaced by sericite and quartz; **(c)** argillization and silicification of volcanic glass in vitric tuff; **(d)** quartz-kaolinite replacement of feldspars, silicification and argillization of groundmass; **(e)** pigmentation of Fe-oxides and primary embayed quartz lined by secondary quartz crystals in silicified and argillizated groundmass; **(f)** silica and clay flooding of matrix and quartz-filled vesicles in the immediate footwall. Abbreviations: Ar– argillization; Fe– iron oxide; F– feldspar (ortoclase); Se– sericitization, Si– silicification; Q– quartz, Op– opaque, V– void.

relative abundances. Footwall dacite consists mainly of Na-Ca smectite, illite, regular and irregular interstratified illite/smectite, interstratified chlorite/smectite and rarely kaolin group minerals (kaolinite and halloysite). The abundances of these minerals change in respect to distance to the ore body. The ore is enveloped by illite and silica minerals. In the footwall, this zone is transitional to illite/smectite and than smectite zone, respectively. Small pockets of the kaolin group minerals are also observed in the smectite zone. The outer zone mainly consists of chlorite and interstratified minerals. Hanging-wall mafic rocks are generally chloritized and partly albitized. Common clay mineralogy in this rock type is chlorite, illite, smectite, irregular interstratified chlorite/smectite.

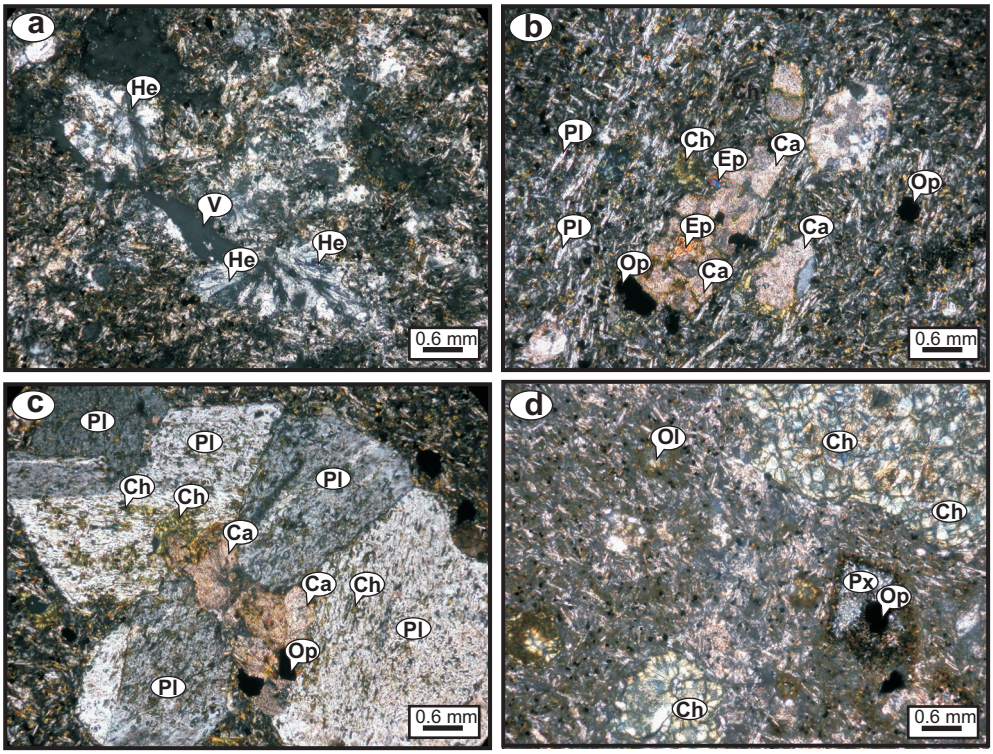

Figure 3. Photomicrographs of hanging wall basalts under crossed polars: **(a)** amygdaloidal zeolite (heulandite) filling; **(b)** calcite and epidote formed on plagioclase; **(c)** Sieve texture in plagioclase and formation of calcite and chlorite on Ca-rich plagioclase; **(d)** skeletal pyroxene and olivine partly converted to chlorite and opaque. Abbreviations: Ca– calcite; Ch– chlorite, Ep– epidote; He– heulandite, Pl– plagioclase, Px– pyroxene; Ol– olivine, V– void.

Similar clay minerals can be observed in altered dolerite dyke, and are composed of chlorite illite/smectite (Figure 4a, b).

Based on clay mineralogy, hydrothermal alteration zones are well developed and represented by silicification-pyrite-illite zone, illite-silicification zone, illite/smectite-silicification zone and smectite zone accompanying kaolinite and halloysite in the footwall rocks, and additionally, chlorite zone in the hanging-wall rocks. In the hanging-wall rocks, zeolite facies minerals such as heulandite, analcime, laumontite and calcite were also determined.

Major element concentrations of purified smectite, kaolinite and illite (<2 μm) and their structural formulae calculated on the basis of 22 oxygen atoms for smectite and illite, and 14 oxygen atoms for kaolinite (Weaver & Pollard 1973; Newman & Brown 1987) are given in Tables 1 and 2. The dioctahedral smectites are rich in Al (22.88 and 23.85 wt% Al_2O_3). The K_2O content is 0.07–0.17 wt% and K as interlayer cation is 0.01–0.03 per unit formulae. These values may not be consistent with general smectite compositions. Interlayer regions are occupied by Ca, Na and K. Octahedral charge of smectites range from 0.36 to 0.45 and tetrahedral charge from 0.06 to 0.14 and tetrahedral/octahedral ratios <1. For this reason, this smectites are classified as montmorillonite (Güven 1988).

The structural formula of kaolinite was calculated from chemical analyses of the clay fractions extracted from sample K40, as given in Table 1. Molar SiO_2/Al_2O_3 ratio is 1.17, total Fe_2O_{3total} content is 1.04 wt%, and MgO content is 1.90 wt% (Tables 1 & 2). Generally it is well known that analysis of an ideal kaolinite does not contain such an amount of iron and magnesium therefore the iron content of kaolinites has been subject of some discussion (Herbillon *et al.* 1976; Rengasamy 1976; Angel & Vincent 1978; Mestdagh *et al.* 1980; Cuttler 1981; Komusinski *et al.* 1981). In the studied kaolinite-

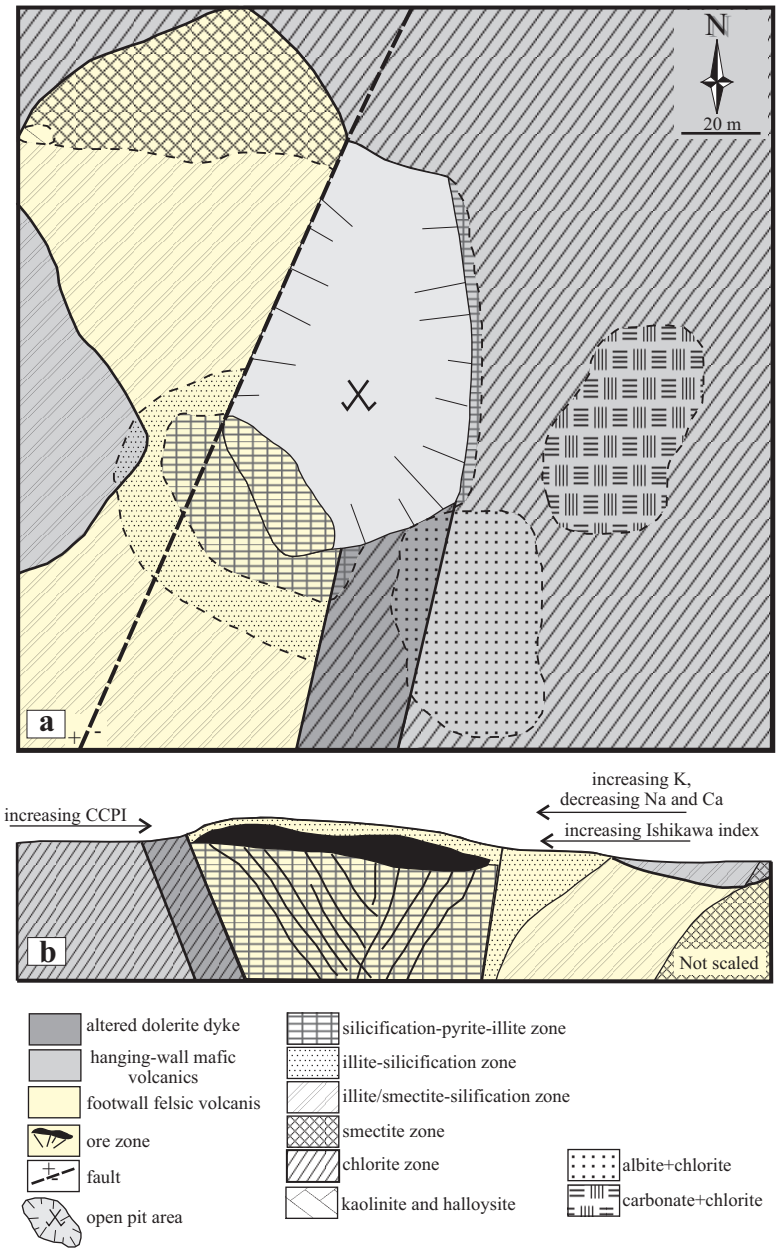

Figure 4. (a) Alteration map of the Kutlular VMS; (b) model of alteration associated with the Kutlular VMS.

rich samples, SEM investigations suggest that amorphous iron coatings are common around the kaolinite fibers and particles and kaolinite are generally derived from the volcanic glass fragments. So that, excess iron content in the chemical analysis of the studied kaolinite may result from iron coatings, and excess magnesium content from the partly dissolved glass that may not be successfully removed with chemical treatments. However, high quality XRD studies (normal, EG solvated, heated) did not show any type of intercalations or impurities. It is suggested that Fe^{3+} and Mg^{2+} might played an important role within the octahedral layers, replacing some of the Al.

K_2O contents of the illites and illite/smectites range from 6.15 to 7.56 wt% and 5.17 to 5.96 wt%, and the

Table 1. Major element (wt%) compositions of clay fraction from the Kutlular area (Sürmene, Trabzon), NE Turkey.

Sample No Mineralogy	KP3-3 Na-Ca S	KP3-5 Ca-S	K40 kaolinite	K33 illite	KP3 illite	KP2a illite/ smectite	KP2-1 illite/ smectite	KP4-7 Ch/S, S	KP3-8 Ca-S, illite. kaolinite	KP1-11 Ch/illite, S, Ch	KP1-11a Ch/illite, S, Ch	KP3-2 Ch/S, Na-S, illite
SiO_2	62.07	62.62	44.55	47.73	49.45	54.31	49.73	48.95	58.04	58.77	62.82	50.05
Al_2O_3	23.85	22.88	37.94	31.53	32.58	27.18	25.94	23.50	16.97	19.19	16.96	26.17
$Fe_2O_3^{total}$	1.63	2.84	1.04	0.67	2.51	1.50	3.83	3.68	7.66	1.21	1.14	3.23
MgO	2.09	1.86	1.90	1.28	1.38	1.07	0.67	0.63	2.14	1.28	1.20	0.63
CaO	1.12	1.040	0.08	0.77	1.20	0.09	0.06	0.11	0.92	0.89	0.77	0.07
Na_2O	1.03	0.51	0.61	0.15	1.15	1.07	0.10	1.03	6.00	4.20	2.88	0.09
K_2O	0.17	0.07	0.04	7.56	6.15	5.17	5.96	3.81	0.350	0.460	0.590	6.060
TiO_2	0.06	0.06	0.53	2.56	0.640	0.70	0.39	0.74	0.480	0.600	0.590	0.570
P_2O_5	0.03	0.04	0.09	0.69	0.000	0.02	0.04	0.02	0.06	0.02	0.02	0.04
MnO	0.01	0.01	0.13	0.01	0.030	0.01	0.01	0.04	0.07	0.02	0.02	0.01
BaO	0.079	0.002	0.053	0.119	0.000	0.106	0.048	0.034	0.027	0.010	0.018	0.050
Cr_2O_3	0.007	0.008	0.013	0.002	<0.01	0.002	0.003	0.001	0.002	0.002	0.002	0.002
LOI	7.89	8.12	14.10	6.50	5.30	8.70	13.10	16.40	7.10	13.20	13.00	12.90
Sum	100.04	100.06	101.08	99.57	100.39	99.93	99.88	98.95	99.82	99.85	100.01	99.87

LOI, represents loss on ignition; Fe_2O_{3total} stands for total iron oxide as ferric iron.
(Abbreviations: Na-Ca-S, Na-Ca smectite; Ca-S, Ca-smectite; Ch, chlorite; S, smectite)

Table 2. Structural formulae of the smectites, illite, illite/smectite and kaolinite of the Kutlular(Sürmene, Trabzon) area (Abbreviations: Na-Ca-S, Na-Ca smectite; Ca-S, Ca-smectite).

Sample No	KP3-3	KP3-5	K40	K33	KP3	KP2a	KP2-1
Mineralogy	Na-Ca-S	Ca-S	kaolinite	illite	illite	illite/smectite	illite/smectite
Tetrahedral							
Si	7.8601	7.9418	3.8521	6.3914	6.4488	7.2188	7.0466
^{IV}Al	0.1399	0.0582	0.1479	1.6086	1.5512	0.7812	0.9534
Sum	8.0000	8.0000	4.0000	8.0000	8.0000	8.0000	8.0000
Octahedral							
^{VI}Al	3.4196	3.3618	3.7185	3.3674	3.4563	3.4767	3.3786
Ti	0.0057	0.0057	0.0345	0.2578	0.0628	0.0700	0.0416
Fe^{3+}	0.1553	0.2710	0.0677	0.0675	0.2463	0.1500	0.4084
Mg	0.3945	0.3516	0.2449	0.2555	0.2682	0.2120	0.1415
Cr	0.0004	0.0004	0.0004	0.0001	0.0000	0.0001	0.0002
P	0.0016	0.0021	0.0033	0.0391	0.0000	0.0011	0.0000
Ba	0.0039	0.0001	0.0018	0.0063	0.0000	0.0055	0.0027
Sum	3.9810	3.9928	4.0000	3.9936	4.0000	3.9154	3.9729
Interlayer							
Ca	0.1520	0.1413	0.0074	0.1105	0.1677	0.0128	0.0091
Na	0.2529	0.1254	0.1023	0.0389	0.2908	0.2758	0.0275
K	0.0275	0.0113	0.0044	1.2914	1.0231	0.8766	1.0773
Mg	0.0000	0.0000	0.0710	0.0000	0.0336	0.0000	0.0000
Sum	0.4323	0.2781	0.1141	1.4408	1.4815	1.1652	1.1139
Si/Al	2.2082	2.3222	0.9963	1.2844	1.2878	1.6954	1.6266
TC	0.1399	0.0582	0.1479	1.6086	1.5512	0.7812	0.9534
OC	0.4465	0.3637	-0.0077	-0.0553	0.1046	0.3991	0.1836
TOT	0.5864	0.4219	0.1402	1.5535	1.6558	1.1803	1.1370
IC	-0.5843	-0.4194	-0.2635	-1.5513	-1.7165	-1.1780	-1.1230

TC, tetrahedral charge; OC, octahedral charge; TOT, Total charge (octahedral charge + tetrahedral charge); IC, interlayer charge

value of K^+ are from 1.02 to 1.29 and from 0.88 to 1.08 moles in formula unit, respectively. CaO contents of the illites and illite/smectite are from 0.77 to 1.20 wt% and 0.06 to 0.09 wt%. Interlayer region is occupied by K^+, Ca^{2+} and Na^+ (Tables 1 & 2).

Whole Rock Geochemistry

Formation of the VMS results in intense alteration and development of alteration haloes around the ore body. Due to strong hydrothermal alteration of footwall and hanging-wall rocks, many of the analyzed elements can not be used for the chemical discrimination of the rock types. However, some of the elements in the footwall and hanging wall rocks are implied to behave immobile (e.g., Ti, Al, Zr) during the generation of ore (MacLean & Kranidiotis 1987; MacLean 1990; Barret *et al.* 1993a, b; Shriver & MacLean 1993; Barret & MacLean 1994). Most of the major and trace elements are not useful for chemical discrimination of the Kutlular volcanics due to the intense hydrothermal alteration. For these reasons, the immobile element (Zr, Ti, Nb, Yr) chemical discrimination diagram of Winchester & Floyd (1977) revised by Pearce (1996) was used (Figure 5; Tables 3 & 4). The lower dacite falls into the andesite-basaltic andesite field, probably due to the slight enrichment of the Y. The footwall dacites scatter on andesite/basalt and rhyolite/dacite fields, probably due to the intense hydrothermal alteration. The hanging-wall rocks fall into basalt, andesite-basaltic andesite and occasionally rhyolite-dacite fields. While interpreting these scattering, it should be taken into account that Y is slightly mobile than Nb whereas Ti and Al are highly immobile elements (MacLean & Kranidiotis 1987; MacLean 1990; Barrett & MacLean 1991; Barrett 1992; Shriver & MacLean 1993; Hill *et al.* 2000). Geochemical affinities of the volcanic rocks are determined by using immobile element binary plot of La-Yb and Zr-Y (Figure 6). The volcanics show similar affinity in both diagrams and are generally transitional between tholeiitic and calc-alkaline in character.

The trace elements patterns of the samples show considerable LILE enrichment (K, Rb, Ba and Th) and depletion in Sr and Ti relative to N-MORB (Figure 7). Normalized trace element pattern may be represented by that of island-arc calc-alkaline volcanics (Pearce 1983). Chondrite-normalized REE patterns of the footwall rocks show marked HREE enrichment, a feature which is

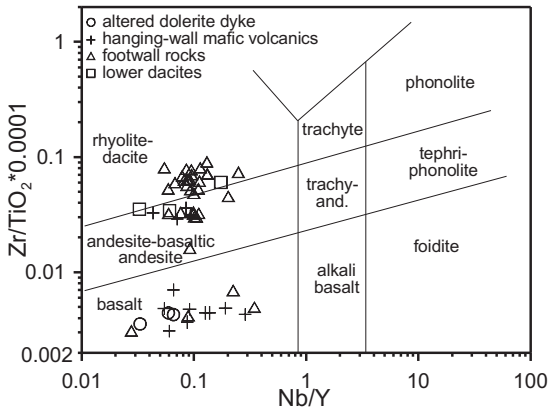

Figure 5. Discrimination of the Kutlular area volcanics using a Nb/Y-Zr/TiO_2 immobile element diagram of Pearce (1996) (after Winchester & Floyd 1977).

common in felsic rocks formed in evolved island arcs (Almodóvar *et al.* 1998). The footwall and hanging-wall rocks have negative and positive Eu and Ce anomalies, respectively, indicating different degree of hydrothermal alteration resulted of interaction with sulphide-sulphate ore forming fluids (Shikazono 2003). Although the negative Eu anomalies in the rocks may reflect plagioclase fractionation in the evolution of the volcanics, it should be kept in mind that Eu content could be diminished due to the hydrothermal breakdown of plagioclase (Shikazono 2003; Figure 8).

Alteration Indices

Ishikawa alteration index (AI) and the chlorite-carbonate-pyrite index (CCPI) track the chemical and mineralogical changes associated with hydrothermal alteration (Ishikawa *et al.* 1976; Large *et al.* 2001). The Ishikawa index ($AI=[100*(K_2O+MgO)]/(K_2O+MgO+Na_2O+CaO)$) was defined by Ishikawa *et al.* (1976) to quantify the intensity of sericite and chlorite alteration that occurs in the footwall volcanic rocks proximal to Kuroko-type VMS deposits. Large *et al.* (2001) imply that the index varies from values of 20 about 60 for unaltered rocks and between 50 and 100 for hydrothermally altered rocks, with an AI= 100 representing complete replacement of feldspar and glass by sericite and/or chlorite. The calculated AI values of the footwall dacites and the lower dacites from the Kutlular mine range from 0.91 to 98.39 and from 16.25 to 94.57, respectively. AI values of hanging mafic volcanics and altered dolerite dyke are 2.38

Table 3. Major (wt%) and trace element (ppm) compositions of the footwall and the lower dacite from the Kutlular (Sürmene, Trabzon) mine. Abbreviations: AI– Ishikawa alteration index, CCPI– Chlorite-carbonate-pyrite index.

	lower dacites			*footwall volcanics*												
	K-26	K-28	K-29	KP1-1	KP1-1*	KP1-2	KP1-3	KP1-4	KP1-5	KP1-7	KP1-8	KP1-9	KP1-10	KP1-11	KP1-12	K40
SiO_2	67.70	70.93	64.72	61.73	47.97	50.30	56.58	74.30	51.83	72.84	92.37	43.75	20.28	50.97	57.63	37.71
Al_2O_3	17.98	13.73	17.44	18.26	21.82	25.46	21.44	2.76	23.92	9.26	3.08	12.72	2.92	25.02	18.38	23.77
$Fe_2O_3^{total}$	4.05	4.47	5.55	4.96	10.97	3.27	3.70	16.98	3.15	1.69	0.83	17.84	38.34	2.52	4.76	12.81
MgO	0.30	0.98	0.56	0.56	1.72	0.88	1.21	0.05	1.05	0.04	0.11	0.91	0.28	0.93	1.44	1.71
CaO	0.01	0.23	0.02	0.20	0.07	0.08	0.03	0.11	0.05	0.29	0.12	0.08	1.53	0.10	0.07	0.19
Na_2O	0.09	5.13	0.04	2.46	0.03	0.90	0.19	0.10	0.45	3.42	0.25	0.33	0.06	0.50	0.11	0.01
K_2O	1.44	0.06	0.07	1.09	4.38	1.97	3.06	0.04	2.91	0.11	0.16	2.24	0.26	2.22	4.16	
TiO_2	0.39	0.39	0.49	0.43	0.28	0.56	0.32	0.19	0.32	2.32	0.08	0.31	0.08	0.32	0.32	0.81
P_2O_5	0.02	0.02	0.03	0.05	0.04	0.04	0.04	0.14	0.04	0.09	0.01	0.02	0.01	0.06	0.01	0.10
MnO	0.01	0.10	0.13	0.02	0.05	0.02	0.03	0.22	0.04	0.02	0.01	0.02	0.01	0.04	0.03	0.26
LOI	8.00	3.90	10.90	10.20	12.50	16.40	13.20	5.00	16.10	9.60	3.00	21.60	36.10	17.10	12.00	21.70
Sum	99.99	99.94	99.95	99.96	99.83	99.88	99.80	99.89	99.86	99.68	100.02	99.82	99.87	99.78	98.91	99.07
FeO^{total}	3.64	4.02	4.99	4.46	9.87	2.94	3.33	15.28	2.83	1.52	0.75	16.05	34.50	2.27	4.28	11.53
Cu	5.10	87.90	334.90	107.90	466.20	116.00	161.60	191.30	150.90	80.30	73.60	53.00	8.10	160.10	35.30	4594.80
Pb	6.00	2.70	2.80	50.60	18.00	89.30	66.80	765.80	106.80	139.90	17.50	59.60	10.70	155.10	15.30	25.60
Zn	8.00	361.00	164.00	27.00	187.00	21.00	43.00	25.00	35.00	6.00	10.00	24.00	37.00	33.00	93.00	1990.00
As	1.90	3.10	3.60	56.90	10.60	133.60	131.70	312.20	139.40	204.40	14.30	387.20	260.20	139.70	62.50	7.40
Ba	239.00	175.10	111.50	333.50	629.20	861.00	1491.70	352.60	777.60	2254.40	154.30	538.00	1341.90	1299.60	8050.50	787.50
Y	37.20	66.90	47.50	25.20	32.00	31.10	27.90	23.10	44.40	16.90	4.90	23.90	3.60	44.20	26.40	18.00
Zr	234.80	136.80	167.40	143.10	253.20	179.40	227.70	117.30	257.30	161.20	36.40	149.80	59.00	247.60	226.50	25.10
Nb	6.50	2.20	2.90	2.50	4.20	3.10	3.70	2.60	5.10	3.80	1.00	2.40	0.90	4.20	3.50	0.50
Rb	19.20	2.30	2.90	25.80	94.70	36.10	57.40	1.10	58.20	3.00	4.30	35.40	4.70	45.10	68.40	1.00
Sr	8.60	54.90	4.50	91.70	6.90	46.10	22.10	36.30	28.20	131.10	33.50	38.50	20.20	34.20	34.30	11.30
Th	5.80	2.30	2.60	1.60	3.80	1.90	3.00	1.60	3.70	2.10	0.90	2.00	0.90	4.50	2.50	0.40
U	1.70	0.40	0.60	2.10	1.00	3.10	1.20	0.90	1.50	5.50	0.50	4.50	3.10	1.90	2.50	0.30
La	2.20	10.20	13.60	6.20	4.70	1.20	1.20	21.90	0.70	1.40	0.70	1.10	1.50	0.80	9.60	4.10
Ce	14.00	16.00	21.30	11.70	13.80	3.80	3.70	47.50	2.80	3.00	2.10	4.20	5.10	2.80	19.20	7.00
Pr	0.70	4.41	5.17	1.16	1.73	0.37	0.31	5.18	0.24	0.32	0.24	0.52	0.73	0.28	2.20	1.01
Nd	3.10	19.80	23.40	4.10	7.40	2.50	2.70	15.50	1.70	1.20	1.10	3.00	3.30	1.80	9.30	4.80
Sm	1.30	6.10	6.30	1.40	3.10	0.80	2.10	4.30	1.00	0.50	0.40	1.10	1.10	0.80	3.10	1.00
Eu	0.26	1.55	1.63	0.28	0.90	0.25	0.48	1.03	0.38	0.07	0.13	0.30	0.41	0.26	0.90	0.42
Gd	2.54	9.03	7.08	1.88	5.32	2.19	4.36	4.04	2.81	1.21	0.57	2.38	1.34	2.77	4.04	1.86
Tb	0.74	1.49	1.23	0.55	1.10	0.53	0.75	0.73	0.93	0.28	0.11	0.67	0.13	0.81	0.78	0.32
Dy	5.29	10.10	7.93	3.98	6.31	4.31	4.80	5.34	6.17	2.09	0.61	3.90	0.65	5.61	5.51	2.27
Ho	1.32	2.13	1.75	0.93	1.34	1.06	0.97	1.15	1.57	0.59	0.16	0.83	0.13	1.49	1.11	0.60
Er	4.32	6.14	5.02	2.95	3.73	3.44	2.83	3.57	4.71	1.95	0.51	2.82	0.44	4.96	3.69	1.56
Tm	0.79	1.07	0.88	0.60	0.67	0.68	0.52	0.60	0.79	0.34	0.09	0.53	0.07	0.77	0.67	0.22
Yb	5.34	6.98	5.10	3.81	4.19	4.89	3.38	3.92	5.00	2.22	0.68	3.43	0.37	4.92	4.27	1.59
Lu	0.80	1.02	0.85	0.66	0.67	0.72	0.54	0.66	0.81	0.38	0.11	0.57	0.07	0.84	0.74	0.27
Nb/Y	0.17	0.03	0.06	0.10	0.13	0.10	0.13	0.11	0.11	0.22	0.20	0.10	0.25	0.10	0.13	0.03
Zr/Y	6.31	2.04	3.52	5.68	7.91	5.77	8.16	5.08	5.80	9.54	7.43	6.27	16.39	5.60	8.58	1.39
Zr/Nb	36.12	62.18	57.72	57.24	60.29	57.87	61.54	45.12	50.45	42.42	36.40	62.42	65.56	58.95	64.71	50.20
AI	94.57	16.25	91.30	38.28	98.39	74.41	95.10	30.00	88.79	3.89	42.19	88.48	25.35	84.00	96.89	89.53
CCPI	72.05	49.08	98.06	58.59	72.44	57.12	58.28	99.09	53.62	30.66	67.64	86.84	99.09	54.03	57.27	99.92
La/Yb	0.41	1.46	2.67	1.63	1.12	0.25	0.36	5.59	0.14	0.63	1.03	0.32	4.05	0.16	2.25	2.58

LOI is loss on ignition, $FeO^{total} = 0.8998 * Fe_2O_3^{total}$ (Ragland 1989).

Table 3. (Continued)

	footwall volcanics															
	KP2-1	KP2-2	KP2-4	KP3-1	KP3-2	KP3-3	KP3-4	KP3-5	KP4-1	KP4-2	KP4-3	KP4-5	K-13	K33	K34	K-37
SiO_2	82.24	73.95	79.66	79.68	81.76	88.62	80.95	85.19	58.71	72.71	74.65	83.33	74.99	45.04	84.27	88.97
Al_2O_3	7.85	4.89	10.75	10.68	5.66	3.82	8.09	3.52	14.90	11.98	10.92	5.69	10.52	18.77	6.99	6.59
$Fe_2O_3^{total}$	3.22	10.68	0.48	0.71	4.63	1.09	3.08	3.01	9.30	2.48	2.73	1.66	0.64	15.17	2.71	0.18
MgO	0.24	0.27	0.39	0.39	0.30	0.05	0.11	0.05	0.49	0.69	0.19	0.30	0.01	0.77	0.27	0.24
CaO	0.05	0.12	0.29	0.16	0.12	0.09	0.05	0.07	0.03	0.70	0.35	0.08	0.14	0.34	0.09	0.01
Na_2O	0.04	0.02	0.04	0.03	0.02	0.04	0.02	0.02	0.08	2.42	0.05	0.07	5.33	0.10	0.04	0.04
K_2O	1.89	1.18	2.00	2.11	1.28	0.13	1.63	0.06	3.46	0.89	2.02	1.45	0.04	5.25	1.89	1.68
TiO_2	0.12	0.09	0.21	0.18	0.09	0.09	0.15	0.07	0.45	0.33	0.32	0.39	3.27	1.77	0.12	0.12
P_2O_5	0.02	0.01	0.01	0.02	0.01	0.02	0.02	0.02	0.02	0.06	0.02	0.14	0.19	0.30	0.01	0.01
MnO	0.01	0.01	0.01	0.01	0.01	0.01	0.01	0.01	0.01	0.01	0.01	0.01	0.01	0.01	0.01	0.01
LOI	4.20	8.70	6.10	5.90	6.00	4.90	5.80	5.50	12.50	7.60	7.70	6.60	4.70	11.20	3.30	2.20
Sum	99.88	99.92	99.94	99.87	99.88	98.86	99.91	97.52	99.95	99.87	24.31	99.72	99.84	98.72	99.70	100.05
FeO^{total}	2.90	9.61	0.43	0.64	4.17	0.98	2.77	2.71	8.37	2.23	2.46	1.49	0.58	13.65	2.44	0.16
Cu	539.10	114.50	5.50	6.60	435.70	112.40	20.40	297.60	226.50	33.40	39.60	201.40	29.60	516.50	1132.90	3.60
Pb	12.80	28.20	79.10	565.10	37.60	35.10	43.60	85.80	12.20	28.90	38.50	1543.10	1316.80	128.90	72.80	8.10
Zn	68.00	67.00	18.00	36.00	139.00	9177.00	310.00	>10000	58.00	227.00	79.00	81.00	3.00	663.00	167.00	2.00
As	18.30	157.30	25.70	55.30	169.20	52.70	112.50	98.50	59.50	53.40	81.30	19.00	108.10	130.90	66.90	145.60
Ba	171.60	88.40	160.10	183.50	141.90	302.40	74.80	29.60	251.10	119.00	173.10	279.70	1438.10	774.90	213.00	144.60
Y	16.70	13.20	19.20	24.90	12.60	11.80	18.40	12.10	24.60	28.40	18.00	29.90	11.20	24.70	16.40	29.30
Zr	75.70	53.80	109.20	126.20	57.10	47.70	85.20	44.10	136.30	106.60	103.70	128.20	162.80	74.20	82.10	96.80
Nb	1.50	0.90	1.80	2.40	1.10	1.30	1.60	1.00	2.50	1.70	2.00	2.30	3.90	2.20	1.30	1.60
Rb	20.10	18.40	20.30	22.70	18.60	1.30	12.50	0.60	38.00	11.20	18.80	16.80	0.70	79.40	24.50	22.40
Sr	4.40	6.20	10.10	14.10	6.80	9.00	2.90	6.30	4.30	77.90	8.40	86.80	73.70	5.10	3.00	3.30
Th	0.80	0.70	1.20	1.80	0.80	0.90	1.60	0.70	1.70	2.20	1.00	1.90	1.30	0.70	1.30	1.00
U	0.30	0.30	0.60	0.60	0.40	0.40	0.50	0.20	0.70	0.30	0.50	1.20	7.30	1.00	2.10	0.40
La	6.10	2.10	4.40	7.60	1.70	5.90	7.20	9.00	6.50	6.00	5.50	33.40	4.30	2.40	4.80	2.50
Ce	13.20	2.90	9.60	17.20	3.30	10.20	14.10	15.00	16.70	15.40	14.20	80.40	7.20	8.50	10.80	6.60
Pr	1.77	0.40	1.29	2.10	0.45	1.49	1.86	2.14	2.34	2.33	2.06	10.91	0.71	1.50	1.73	0.93
Nd	6.50	1.80	4.80	9.90	1.80	5.80	7.90	9.00	8.00	11.20	9.00	46.40	2.30	7.50	6.70	4.10
Sm	2.50	0.70	1.50	2.20	1.30	2.00	2.50	2.10	2.40	3.10	2.20	11.50	0.80	2.60	1.70	1.80
Eu	0.27	0.55	0.31	0.39	0.28	0.68	0.62	0.70	0.55	0.77	0.48	1.94	0.14	0.43	0.31	0.40
Gd	2.04	1.67	1.67	2.59	1.24	1.84	2.72	1.99	2.82	4.17	1.63	8.77	0.89	4.22	1.87	3.09
Tb	0.36	0.28	0.42	0.65	0.28	0.30	0.47	0.32	0.45	0.72	0.36	1.22	0.20	0.64	0.31	0.65
Dy	3.03	2.17	2.59	4.38	1.81	1.79	3.39	1.90	3.87	4.63	2.76	7.16	1.48	4.31	2.70	4.39
Ho	0.59	0.45	0.70	0.76	0.44	0.45	0.73	0.43	0.81	0.90	0.53	1.02	0.40	0.93	0.61	0.95
Er	2.06	1.61	2.34	3.14	1.44	1.27	2.19	1.35	3.16	3.05	2.05	3.33	1.28	2.59	2.00	2.86
Tm	0.36	0.22	0.44	0.45	0.27	0.23	0.32	0.24	0.51	0.44	0.32	0.46	0.23	0.41	0.28	0.49
Yb	2.04	1.97	2.75	3.68	1.75	1.37	2.16	1.56	3.53	3.38	2.49	3.49	1.78	2.54	2.16	3.39
Lu	0.31	0.22	0.40	0.51	0.22	0.21	0.30	0.24	0.49	0.46	0.42	0.58	0.32	0.41	0.31	0.54
Nb/Y	0.09	0.07	0.09	0.10	0.09	0.11	0.09	0.08	0.10	0.06	0.11	0.08	0.35	0.09	0.08	0.05
Zr/Y	4.53	4.08	5.69	5.07	4.53	4.04	4.63	3.64	5.54	3.75	5.76	4.29	14.54	3.00	5.01	3.30
Zr/Nb	50.47	59.78	60.67	52.58	51.91	36.69	53.25	44.10	54.52	62.71	51.85	55.74	41.74	33.73	63.15	60.50
AI	95.95	91.19	87.87	92.94	91.86	58.06	96.13	55.00	97.29	33.62	84.67	92.11	0.91	93.19	94.32	97.46
CCPI	61.91	89.17	28.72	32.47	77.45	85.84	63.59	97.18	71.45	46.88	56.11	54.13	9.84	72.94	58.39	18.94
La/Yb	2.99	1.07	1.60	2.07	0.97	4.31	3.33	5.77	1.84	1.78	2.21	9.57	2.42	0.94	2.22	0.74

LOI is loss on ignition, $FeO^{total}=0.8998*Fe_2O_3^{total}$ (Ragland 1989).

Table 4. Major and trace element compositions of the hanging-wall mafic volcanics and the altered dolerite dike from the Kutlular (Sürmene, Trabzon) mine. Abbreviations: AI– Ishikawa alteration index, CCPI– Chlorite-carbonate-pyrite index.

	hanging-wall mafic volcanics										*altered dolerite dyke*		
	K-8	K-20	K-27	KUPA1-1	KUPA1-3	KUPA3-6	KP3-6	KP3-7	KP3-8	KP4-6	K24	K-17	K-18A
SiO_2	56.17	54.00	61.20	58.74	51.32	72.80	71.88	65.90	70.79	71.40	50.34	54.31	55.75
Al_2O_3	18.46	16.05	20.39	14.07	14.46	13.50	14.11	16.83	13.31	12.91	15.95	15.17	15.14
$Fe_2O_3^{total}$	7.61	9.74	5.02	8.52	13.71	2.72	2.76	4.52	4.09	2.52	10.11	11.78	9.01
MgO	3.14	3.33	0.07	3.93	6.03	0.69	0.72	0.19	1.05	0.03	7.11	3.80	3.29
CaO	0.21	4.56	0.03	3.48	4.31	0.64	0.64	0.76	0.45	3.57	8.37	5.25	4.20
Na_2O	6.10	5.35	0.02	4.41	2.71	4.85	4.89	5.62	6.07	3.41	2.41	3.37	5.49
K_2O	0.04	0.04	0.08	0.01	0.11	1.02	1.20	0.06	0.16	0.14	0.09	0.14	0.26
TiO_2	1.56	1.37	0.44	1.09	1.51	0.36	0.39	0.45	0.37	0.38	0.61	1.34	1.39
P_2O_5	0.23	0.27	0.06	0.26	0.20	0.06	0.06	0.04	0.03	0.06	0.07	0.29	0.27
MnO	0.19	0.14	0.05	0.10	0.15	0.09	0.09	0.08	0.08	0.05	0.18	0.22	0.36
LOI	6.20	5.10	12.50	5.40	5.50	3.20	3.10	5.40	3.40	5.30	3.50	4.30	4.80
Sum	99.91	99.95	99.86	100.01	100.01	99.93	99.84	99.85	99.80	99.77	98.74	99.97	99.96
FeO^{total}	6.85	8.76	4.52	7.67	12.34	2.45	2.48	4.07	3.68	2.27	9.10	10.60	8.11
Cu	498.00	13.40	110.50	16.90	24.30	71.50	49.70	85.60	145.00	16.20	88.00	17.30	26.60
Pb	76.50	1.80	790.10	1.50	3.40	3.40	3.90	8.20	3.00	6.10	2.80	1.60	1.20
Zn	610.00	110.00	936.00	68.00	121.00	255.00	352.00	166.00	479.00	330.00	59.00	89.00	100.00
As	36.50	10.40	5.30	1.50	6.00	4.30	5.30	7.10	5.90	10.60	6.90	4.00	4.90
Ba	78.60	126.00	193.00	115.40	75.50	287.70	286.10	101.90	109.00	935.60	183.70	156.80	200.40
Y	17.10	31.10	27.30	28.70	21.40	26.90	24.50	26.70	25.20	20.90	15.00	28.50	27.20
Zr	57.50	66.30	136.00	76.40	46.70	129.90	123.10	138.20	107.00	118.10	21.70	59.40	59.50
Nb	1.50	1.70	2.60	1.90	1.30	2.30	2.30	2.50	1.80	2.00	0.50	1.70	1.80
Rb	0.60	0.80	1.60	<.5	0.60	16.20	16.70	0.70	4.40	<.5	0.80	2.00	4.30
Sr	63.80	313.90	22.00	142.70	137.90	207.40	202.10	37.60	59.90	57.20	274.90	268.70	296.30
Th	0.60	0.60	1.90	0.20	0.40	1.70	1.30	20.00	1.50	1.60	0.40	0.50	0.60
U	1.40	0.60	0.80	0.50	0.30	0.50	0.50	0.80	0.40	0.60	0.10	0.20	0.30
La	3.40	6.10	18.00	5.00	3.60	4.30	4.20	8.80	5.70	7.20	1.90	4.70	4.20
Ce	11.20	14.90	41.30	14.90	9.60	11.30	10.10	24.10	9.50	14.80	4.90	13.50	12.90
Pr	1.69	2.22	6.59	2.15	1.42	1.48	1.38	2.78	1.93	1.93	0.83	2.22	1.99
Nd	10.20	11.60	26.30	10.30	7.40	6.50	6.80	11.00	10.10	8.40	4.90	11.40	9.80
Sm	3.20	3.60	6.10	3.30	2.30	2.10	2.10	3.00	2.50	2.20	1.30	3.10	3.40
Eu	1.32	1.57	1.41	1.09	0.97	0.47	0.55	0.73	0.55	0.60	0.68	1.60	1.35
Gd	4.07	4.75	5.17	4.25	3.07	2.78	3.09	2.87	3.33	2.87	2.23	4.91	4.44
Tb	0.73	0.83	0.90	0.84	0.61	0.64	0.65	0.54	0.53	0.48	0.37	0.80	0.78
Dy	3.52	5.03	5.33	4.74	3.21	3.85	3.95	4.33	3.87	3.20	2.78	4.87	4.64
Ho	0.71	1.11	0.98	0.98	0.80	0.90	0.70	0.95	0.78	0.65	0.58	1.03	0.95
Er	1.80	3.12	2.99	2.78	2.16	2.78	2.84	3.28	2.73	2.45	1.50	2.97	2.79
Tm	0.27	0.65	0.46	0.50	0.35	0.51	0.53	0.57	0.42	0.37	0.23	0.48	0.45
Yb	1.44	2.84	3.60	2.63	1.92	2.90	3.62	3.90	2.88	2.91	1.44	2.88	2.38
Lu	0.31	0.47	0.54	0.42	0.33	0.50	0.49	0.57	0.45	0.40	0.27	0.42	0.39
Nb/Y	0.09	0.05	0.10	0.07	0.06	0.09	0.09	0.09	0.07	0.10	0.03	0.06	0.07
Zr/Y	3.36	2.13	4.98	2.66	2.18	4.83	5.02	5.18	4.25	5.65	1.45	2.08	2.19
Zr/Nb	38.33	39.00	52.31	40.21	35.92	56.48	53.52	55.28	59.44	59.05	43.40	34.94	33.06
AI	33.51	25.38	75.00	33.25	46.66	23.75	25.77	3.77	15.65	2.38	40.04	31.37	26.81
CCPI	61.93	69.17	97.87	72.45	86.69	34.83	34.47	42.84	43.16	39.29	86.64	80.40	66.47
La/Yb	2.36	2.15	5.00	1.90	1.88	1.48	1.16	2.26	1.98	2.47	1.32	1.63	1.76

LOI is loss on ignition, $FeO^{total} = 0.8998 * Fe_2O_3^{total}$ (Ragland 1989).

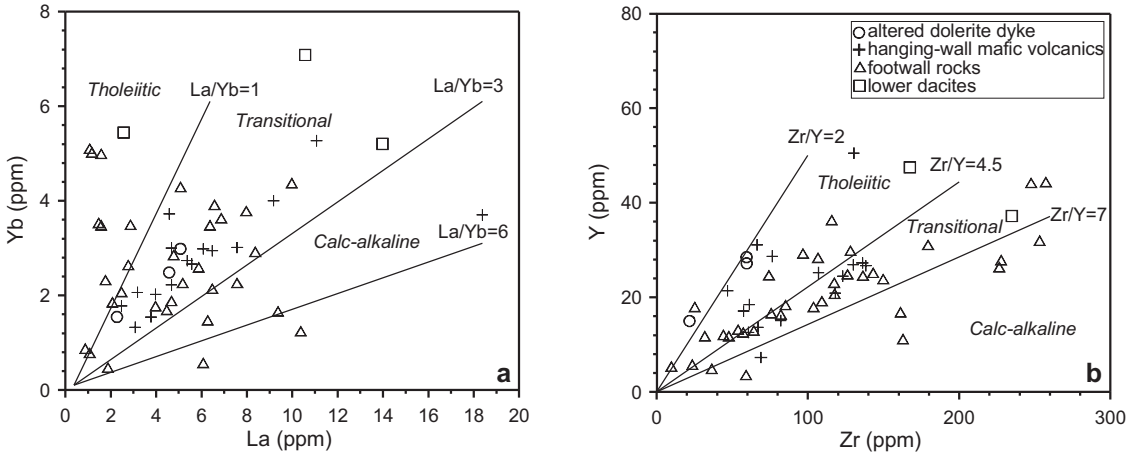

Figure 6. Geochemical affinities of the Kutlular area volcanics (a) La versus Yb plot and (b) Zr versus Y plot. Discrimination lines from Barret & MacLean (1994, 1999).

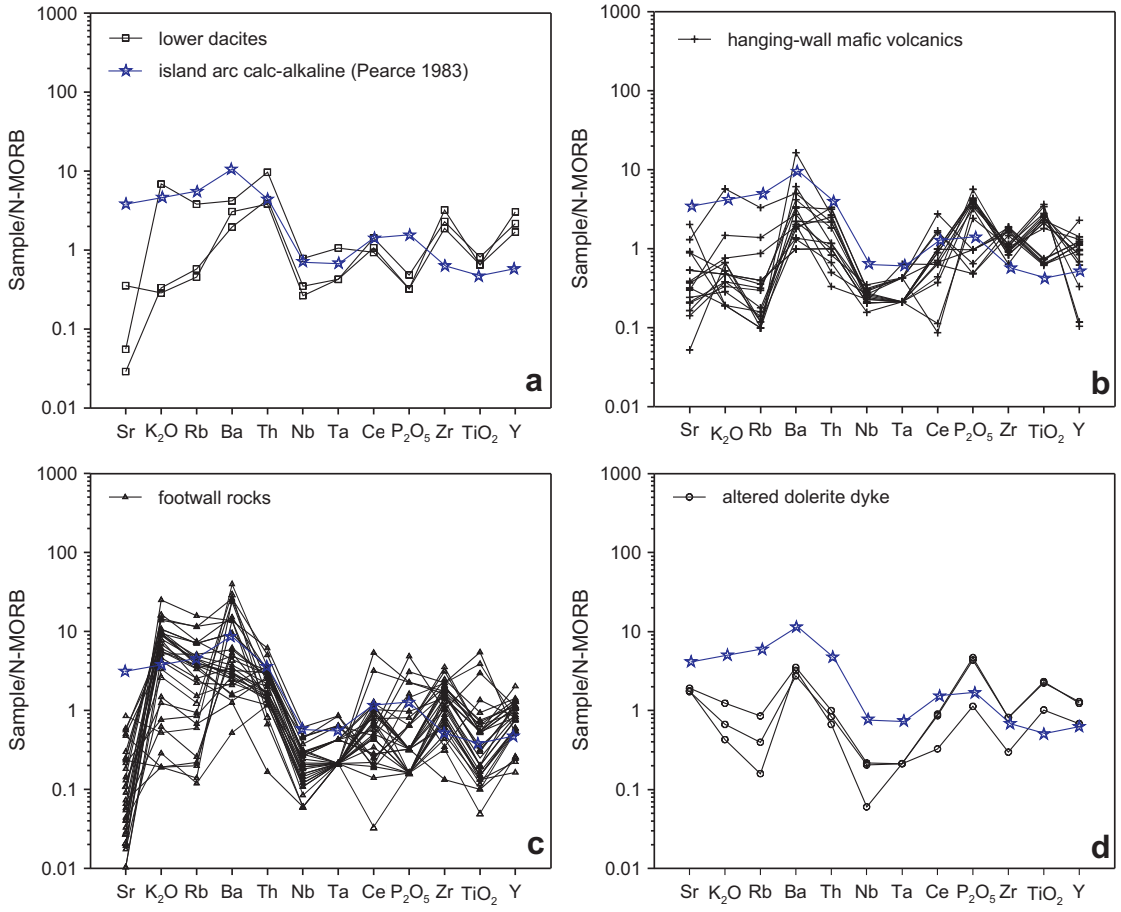

Figure 7. Spider diagrams of the Kutlular volcanics normalized to N-type MORB (normalizing values from Sun & McDonough 1989).

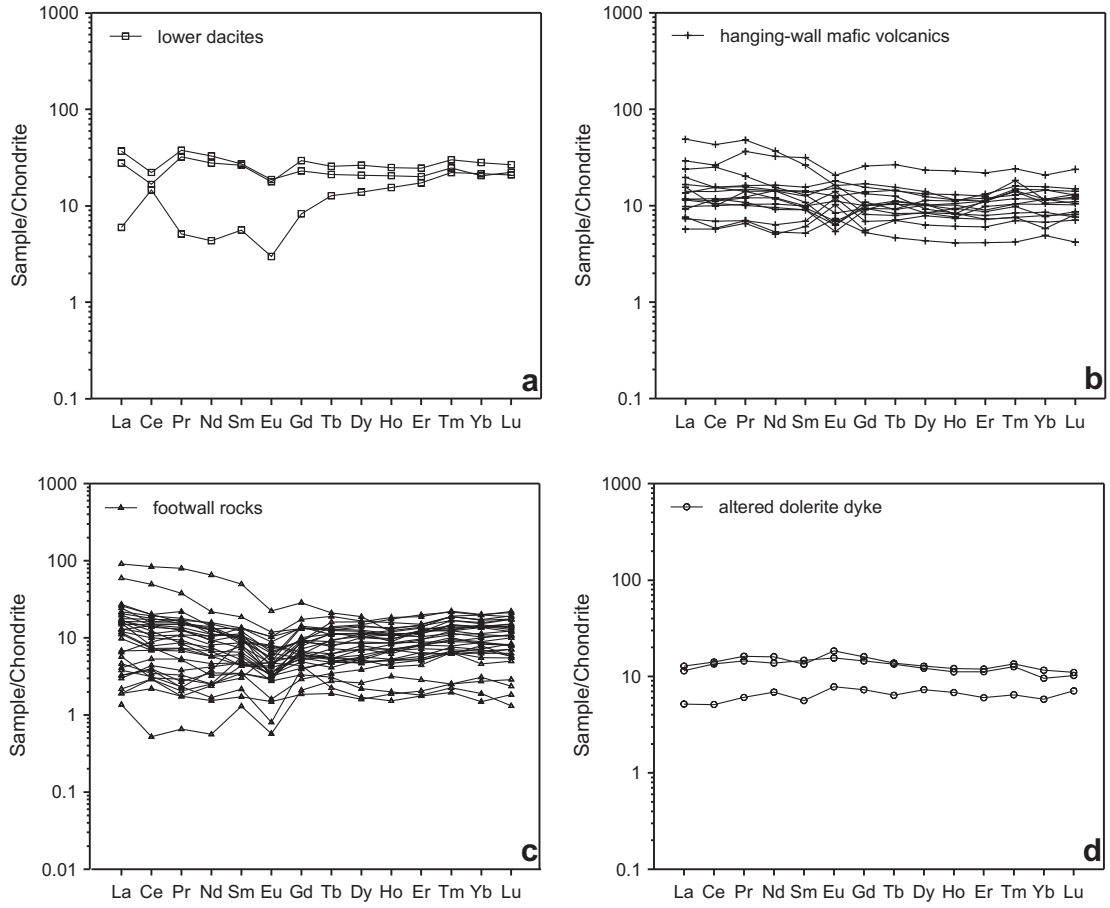

Figure 8. REE patterns of the Kutlular volcanics normalized to chondrite values (Taylor & McLennan 1985) showing enrichment and depletion of REE during the alteration processes.

to 75. In the all types of rock from the study area, AI values increase towards the ore horizon that is consistent with mineralogical observations. High AI values may be due to the breakdown of plagioclase, volcanic glass and their replacement by illite (Tables 3 & 4).

The Ishikawa index has two limitations: (i) it does not enable separation of chlorite-from sericite-rich alteration and (ii) it does not consider carbonate alteration. For these reasons, the chlorite-carbonate-pyrite index (CCPI= $100*(MgO+FeO_{total})/(MgO+FeO_{total}+Na_2O+K_2O)$ were used to distinguish samples with high chlorite content. CCPI values of hanging wall mafic volcanics and altered dolerite dyke fluctuate between 34.47 and 97.87 and footwall volcanics range from 9.84 to 99.92 (Tables 3 & 4). Hanging wall mafic rocks and footwall felsic rocks generally have high CCPI values, indicating the importance of chlorite and pyrite formation in these rocks.

Mass Balance Calculations

During alteration, some elements are mobile whereas others are relatively immobile and become enriched in the residual rock. The extent of element mobility during alteration of the footwall and hanging-wall rocks of massive ore can be estimated using the method of MacLean & Kranidiotis (1987). Mass changes in hydrothermal alteration zones associated with VMS deposits yield quantitative information on hydrothermal alteration and fluid-rock interaction. Immobile element geochemical methods allow the determination of primary fractionation trends in volcanic rocks, subsequent mass changes, and the recognition of volcanic units in altered sequences. Although the method does not consider neither possible change in the density of the primary rock nor changes in the primary rock volume (MacLean 1990),

the mass-balance calculations can be used to identify the relative gains or losses of elements during ore formation.

All the rock samples (Tables 3 & 4) analyzed were separated into 4 main types of alteration groups, based on petrographic studies, chemical and XRD analyses. These are illite zone, chlorite zone, interstratified illite/smectite zone and smectite zone. In the footwall dacite, illite zone, interstratified illite/smectite zone with silicification, and smectite zone were observed from central part to outer zone of ore whereas in the hanging-wall rocks chlorite alteration is common. These alteration groups were also examined by means of mass balance calculations using the MINSQ computer program (Hermann & Berry 2002; Table 5). Mass change calculations were applied to groups of different alteration mineralogy in footwall and lower dacites using single precursor method of MacLean and Kranidiotis (1987). In the calculations, Zr owing to its immobile character and high correlation coefficients with the other elements, and the least altered dacite composition of Akçay (2008) due to the lack of fresh footwall dacite composition in the studied area were used. The least altered dacite composition of Akçay (2008) is the mean of ten dacites, collected from footwall rocks of eastern Pontide massive sulfide deposits and is stratigraphically equivalent to those of Kutlular area (Table 6, Figure 9). For the mass-balance calculations, the means of anhydrous equivalent of these groups are recalculated. The equation used in the calculations can be written for SiO_2 as follows (MacLean & Kranidiotis 1987):

$$SiO_2 = \frac{SiO_2\,(Wt\%)}{Zr\,(ppm)}\,(alt.rock) \times Zr\,(ppm - freshrock)$$

Using the above equation, calculations were done for each element (RC) and in order to determine mass gains and losses (ΔC_i), least altered dacite composition are subtracted from the values of RC.

Hydrothermal alteration around the Kutlular VMS deposit caused mass increases within the illite/smectite zone and the illite zone with silicification, whereas decreases can be noted within smectite zone of the footwall dacite and lower dacites (Table 6). Overall, REE were depleted within footwall and lower dacites. The illite zone is characterized by SiO_2 and $Fe_2O_3^{total}$ increases of 99.68 and 6.40 g/100 g rock, respectively. CaO and Na_2O were depleted while K_2O was enriched, owing to sericitization of plagioclase. In this zone, the total mass gain is 105.36 g/100 g rock, which is met by addition of quartz and pyrite. Mobile trace elements increased significantly, with the highest change in Cu (762.56 g/100 g rock). Ba considerably was depleted, probably due to the complete destruction of feldspar. The illite/smectite interstratified clay mineral zone exhibit similar characteristics but different degree of enrichments or depletions. Mass gain in this group is 54.97 g/100 g. Except for SiO_2 and $Fe_2O_3^{total}$, all other major elements were slightly depleted. Changes in relative abundances of CaO and Na_2O may be interpreted as alkali element leaching in spite of the fact that these elements were taken up during smectite formation. Smectitic alteration resulted in a significant decrease in SiO_2. In the lower dacites, SiO_2 is depleted while Al_2O_3 and $Fe_2O_3^{total}$ were enriched due to the argillization and hematitization. During the hydrothermal alteration Zr and Nb behave immobile but Y is generally mobile in character.

Table 5. Calculated mineralogical compositions using the MINSQ method of Hermann & Berry (2002) from major element chemistry (Tables 3 & 4) of groups of footwall and hanging wall mafic volcanics with similar hydrothermal alteration pattern.

	footwall volcanics			*hanging-wall mafic volcanics*	
	smectite zone	illite/smectite zone	illite zone + silicification	Fe-rich chlorite	Mg-rich chlorite
	Mean (5)	Mean (5)	Mean (6)	Mean (8)	Mean (4)
quartz	22.95	55.97	68.26	20.16	23.62
smectite	34.05	0.02	0.00	4.44	5.15
kaolinite	19.29	0.58	0.00	8.69	13.30
illite	0.00	0.52	18.72	3.50	0.85
illite/smectite	0.00	9.88	1.81	2.27	2.15
Fe-chlorite	0.00	0.57	0.00	7.83	4.53
Mg-chlorite	0.00	0.00	0.00	1.34	6.49
tosudite	0.00	0.00	0.00	0.36	0.17
palygorskite	0.00	0.23	0.00	0.00	0.00
albite	4.00	5.48	0.00	26.27	28.46
anorthite	0.01	0.01	0.00	4.55	0.00
K-feldspar	10.41	1.90	2.90	0.62	0.00
augite	0.00	0.00	0.00	12.40	6.07
pyrite	0.60	12.46	5.41	0.06	0.03
hematite	2.21	3.30	0.05	0.00	2.12
ilmenite	0.00	0.00	0.00	1.68	1.44
epidote	0.00	0.00	0.00	1.60	1.95
accessory	0.34	1.95	0.30	0.32	0.04
sum	93.87	92.86	97.46	96.08	96.34
res SSQ	0.22	0.62	0.12	0.09	0.14

Table 6. Average chemical compositions of groups of footwall rocks with similar hydrothermal alteration pattern, and their reconstructed compositions (RC) and net mass changes (ΔC_i) calculated using the method of MacLean & Kranidiotis (1987). Compositional values for the oxides are in % and all other elements in ppm, and mass changes for them are in g/100g rock and in ppm/100 g rock, respectively. The least altered dacite composition is from Akçay (2008).

	lower dacites				footwall volcanics								
	least altered	lower dacites	RC	ΔC_i	smectite zone	RC	ΔC_i	I/S zone	RC	ΔC_i	illite zone	RC	ΔC_i
SiO_2	75.77	73.39	72.12	-3.65	70.99	66.66	-9.11	76.88	119.14	43.37	85.43	175.45	99.68
Al_2O_3	12.47	17.74	17.43	4.96	20.91	19.64	7.17	6.74	10.45	-2.02	7.83	16.07	3.60
$Fe_2O_3^{total}$	2.61	5.08	4.99	2.38	3.61	3.39	0.78	13.47	20.87	18.26	4.39	9.01	6.40
MgO	0.89	0.66	0.65	-0.24	0.86	0.81	-0.08	0.19	0.29	-0.60	0.28	0.57	-0.32
CaO	1.95	0.09	0.09	-1.86	0.11	0.10	-1.85	0.50	0.77	-1.18	0.13	0.26	-1.69
Na_2O	3.59	1.90	1.87	-1.72	0.96	0.91	-2.68	0.84	1.30	-2.29	0.03	0.07	-3.52
K_2O	2.24	0.57	0.56	-1.68	2.09	1.96	-0.28	0.61	0.94	-1.30	1.75	3.59	1.35
TiO_2	0.33	0.46	0.45	0.12	0.39	0.36	0.03	0.65	1.01	0.68	0.14	0.28	-0.05
P_2O_5	0.07	0.03	0.02	-0.05	0.04	0.04	-0.03	0.06	0.10	0.03	0.01	0.03	-0.04
MnO	0.07	0.09	0.09	0.02	0.03	0.03	-0.04	0.06	0.10	0.03	0.01	0.02	-0.05
Cr_2O_3	0.00	0.00	0.00	0.00	0.01	0.01	0.01	0.00	0.00	0.00	0.00	0.00	0.00
Sum	100.00	100.00	98.27	-1.73	100.00	93.91	-6.09	100.00	154.97	54.97	100.00	205.36	105.36
Cu	6.90	188.48	185.22	178.32	127.94	120.15	113.25	112.18	173.84	166.94	374.68	769.46	762.56
Pb	10.70	3.11	3.06	-7.64	206.00	193.45	182.75	159.84	247.70	237.00	45.68	93.82	83.12
Zn	68.90	234.22	230.17	161.27	23.60	22.16	-46.74	2204.20	3415.78	3346.88	128.17	263.21	194.31
As	5.40	3.19	3.13	-2.27	131.28	123.28	117.88	125.62	194.67	189.27	91.65	188.22	182.82
Ba	468.70	153.93	151.27	-317.43	723.62	679.55	210.85	886.96	1374.49	905.79	141.63	290.86	-177.84
Y	34.40	54.98	54.03	19.63	26.70	25.07	-9.33	16.06	24.89	-9.51	16.08	33.03	-1.37
Zr	158.50	161.29	158.50	0.00	168.78	158.50	0.00	102.28	158.50	0.00	77.18	158.51	0.01
Nb	5.80	2.99	2.94	-2.86	3.08	2.89	-2.91	2.20	3.41	-2.39	1.37	2.81	-2.99
La	17.10	10.82	10.64	-6.46	2.00	1.88	-15.22	7.66	11.87	-5.23	4.38	9.00	-8.10
Ce	29.30	18.13	17.82	-11.48	4.82	4.53	-24.77	16.60	25.72	-3.58	8.98	18.45	-10.85
Pr	4.20	4.34	4.26	0.06	0.46	0.44	-3.76	1.96	3.04	-1.16	1.25	2.57	-1.63
Nd	18.80	19.54	19.21	0.41	2.42	2.27	-16.53	7.14	11.06	-7.74	4.92	10.10	-8.70
Sm	4.30	5.66	5.56	1.26	1.14	1.07	-3.23	2.02	3.13	-1.17	1.70	3.49	-0.81
Eu	1.00	1.44	1.42	0.42	0.30	0.29	-0.71	0.52	0.80	-0.20	0.39	0.80	-0.20
Gd	5.00	7.44	7.31	2.31	2.36	2.22	-2.78	2.20	3.42	-1.58	1.87	3.84	-1.16
Tb	6.20	1.29	1.27	-4.93	0.57	0.54	-5.66	0.42	0.65	-5.55	0.35	0.73	-5.47
Dy	6.20	8.60	8.45	2.25	3.97	3.73	-2.47	2.85	4.42	-1.78	2.62	5.37	-0.83
Er	4.20	5.44	5.35	1.15	2.89	2.71	-1.49	2.07	3.21	-0.99	1.94	3.98	-0.22
Yb	4.20	5.96	5.86	1.66	3.55	3.34	-0.86	2.31	3.58	-0.62	2.14	4.39	0.19
Lu	0.70	0.92	0.90	0.20	0.57	0.53	-0.17	0.37	0.57	-0.13	0.29	0.60	-0.10
Total REE				-13.16			-77.66			-29.72			-37.88

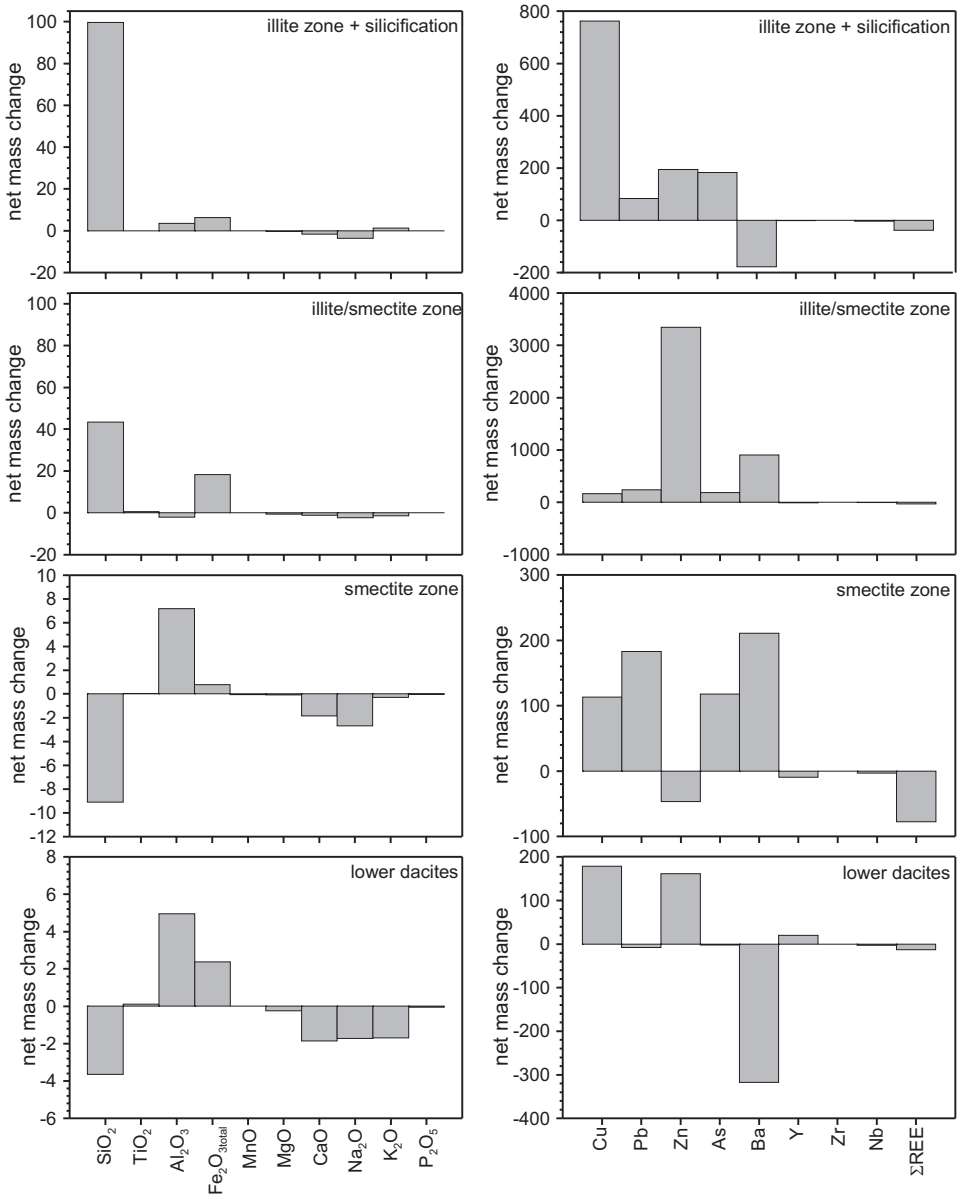

Figure 9. Bar plots showing average net mass changes for grouped rocks regarding clay mineralogy and degree of alteration. In calculations, the method of MacLean & Kranidiotis (1987) and the least altered dacite composition of Akçay (2008) were used. Values are g/100 g for the major oxides, and in ppm/100 g for trace elements.

Discussion

The argillic zones of the massive sulfide alteration haloe contain mixed layer illite/smectite, illite, Fe-Mg chlorite and kaolin group minerals and are characterized by transformations in the mixed layer and the kaolinite polytypes with proximity to the orebodies (Inoue & Utada 1983; Inoue *et al.* 1988; Marumo 1989). In the footwall felsic rocks of the Kutlular area, occurrences of interstratified illite/smectite (I/S), which are characteristic minerals of neutral to alkaline types of alteration in felsic rocks (Inoue 1995), may be considered intermediate products in the smectite to illite sequence of mineral

transformation as a result of increasing temperature towards the ore horizon. Since illite's stability temperature ranges from about 200° to 300 °C, it can be used as a geothermometer of prograde thermal effects. At temperatures less than about 200 °C, interlayered illite/smectite or discrete smectite prevails and may overprint pre-existing illite. Besides, illite forms in the presence of weakly acidic (CO_2-rich) fluids (Steiner 1968; Horton 1985; Simmons & Browne 1990).

In the alteration haloes of the Kutlular area, kaolin group minerals accompany the smectite within the marginal argillic zone, and these are not observed within the inner alteration horizon. It is known that kaolin group minerals form under low-temperature conditions (<150–200 °C) and are indicative of formation at a pH of around 3-4 (Hemley *et al.* 1980; Sillitoe 1993; Arribas 1995). The alteration mineral paragenesis of the Kutlular area suggest that the hydrothermal solutions were acidic during the formation of the ore body, kaolinite-halloysite and illite zones, but became alkaline with decreasing temperature towards to the end of ore deposition.

In the Kutlular area, the chlorite alteration occupies typically the innermost alteration zone, and passes outward into the illite alteration. The basaltic and basaltic andesites around the ore body contain chlorite accompanying epidote and albite, indicating an alteration temperature around 200 °C (i.e. Inoue 1995). Chlorite was observed as replacements of mafic phenocrysts, glass and void infillings. It is possible to see chlorite also as inclusion in albitized plagioclase. In the studied deposit, the composition of chlorite may vary from Fe-rich adjacent to massive sulphide mineralization, to Mg-rich on the periphery of mineralized zones. This occurs particularly in Precambrian deposits, whereas younger deposits may be dominated by Mg-rich chlorite. Mg-rich chlorite is considered to result from the interaction of cold seawater with hot hydrothermal fluids (Allen 1988; Franklin *et al.* 1981; Santaguida *et al.* 1992). In case of the high Fe/Mg ratio, glass, plagioclase and sericite are converted to chlorite (Barrett & MacLean 1994). This process can be formulated by the chemical reaction given by Large *et al.* (2001) as follows:

$$\underset{\text{albite}}{3NaAl_3Si_3O_8} + K^+ + 2H^+ \longrightarrow \underset{\text{sericite}}{KAl_3Si_3O_{10}(OH)_2} + 6SiO_2 + 3Na^+$$
quartz

$$\underset{\text{sericite}}{2KAl_3Si_3O_{10}(OH)_2} + 3H_4SiO_4 + 9Fe^{+2} + 6Mg^{+2} + 18H_2O \longrightarrow \underset{\text{chlorite}}{3Mg_2Fe_3Al_2Si_3O_{10}(OH)_8} + 2K^+ + 28H^+$$

Using these reaction, it can be easily explained why illite were rarely seen in the chlorite zone of the studied area (e.g., Sangster 1972; Lydon 1988; Large 1992; Lentz 1999; Schardt *et al.* 2001). With decreasing temperature, chlorite gradually changes to chlorite/smectite, illite/smectite and smectite towards to the outer zone away from the ore body.

The zeolites which are commonly present in the hydrothermal systems can be classified as Na, Ca- and Ca-Mg series of alteration (Inoue 1995). In the studied area, mordenite, heulandite, stilbite, laumontite and analcime are determined which characterize the Ca- and Na-type of alteration. With decreasing temperature, Ca-zeolites (laumontite, heulandite, stilbite) and Na-zeolite (analcime) are determined from centre to margin of the ore horizon as void infillings and replacement of plagioclase. Na-type alteration is reported by Utada & Ishikawa (1973) at the marginal zones in some Kuroko-type alteration with extensive occurrences of analcime and Na-smectite.

Textural (e.g., Khin & Large 1992; Sharpe & Gemmell 2001) and chemical evidence (e.g., Herrmann & Hill 2001; Large *et al.* 2001) imply that direct precipitation is not as important as void infilligs and selective replacements of the volcanic components on the sea floor. In these cases, formation of carbonate minerals involves mixing of hydrothermal fluids and seawater below the sea floor in permeable volcanic units (e.g., Hermann & Hill 2001). It is also reported that the carbonate formation results from a mixing of small amounts of magmatic CO_2-rich fluid with seawater at or below the palaeo-sea floor (Khin Zaw & Large 1992; Callaghan 2001). In the study area, calcite is determined in the chlorite zone close to the ore within the fracture and pores of the basalt and basaltic andesite, and has low intensity. The source of Ca might be plagioclase and Ca-rich clinopyroxene. The formation of calcite can be explained by the following reaction:

$$CaO + CO_2 + H^+ + OH^- \longrightarrow \underset{\text{calcite}}{CaCO_3} + H_2O$$

Calculated mass changes in the footwall dacites commonly are large, and result from major silica mass transfer. Mass-change calculations indicate that CaO + Na_2O + MgO were leached from the rocks by hydrothermal solutions, whereas large amounts of hydrothermal Fe_2O_{3total} were added. Hanging wall basalt and basaltic andesite show mass changes that are generally much smaller than in the footwall.

Conclusions

Alteration geology, mineralogy and geochemistry studies of the Kutlular (Sürmene, Trabzon) area reveals following findings:

(1) The mineralogic and petrographic investigations of the Kutlular massive sulphide deposit footwall and hanging-wall rocks reveal that smectite, illite/smectite, illite and chlorite are abundant clay minerals to proximity of the ore. The other clay minerals are kaolinite and chlorite/smectite. All these hydrothermal mineral assemblages are accompanied by silica polymorphous.

(2) The clay mineralogy studies indicate that silicification+pyrite+illite zone, illite+silicification zone, illite/smectite+silification zone and smectite zone accompanying kaolinite and halloysite are present in the footwall rocks whereas chlorite zone is well developed in the mafic volcanics.

(3) Immobile trace and rare-earth element data indicate that the footwall and hanging-wall volcanic rocks transitional between tholeiitic and calc-alkaline in character. The trace elements patterns of the samples show considerable LILE enrichment (K, Rb, Ba) and depletion in Sr, La and Ti relative to N-MORB.

(4) Chondrite-normalized REE patterns of the volcanics show a pronounced HREE enrichment. Additionally, the volcanic rocks have different degree of positive and negative Eu and Ce anomalies implying different degree of hydrothermal alteration resulted of interaction with sulphide-sulphate ore forming fluids.

(5) The Kutlular area footwall and hanging-wall alteration zones have several geochemical characteristics that show systematic changes with increasing proximity to the ore. These include Na depletion and elevated alteration index (AI), chlorite-carbonate-pyrite index (CCPI).

Acknowledgements

This paper is a part of PhD study of the first author, and supported by Karadeniz Technical University Scientific Research Fund (Project 2005.112.005.3). The authors thank to Nilgün Güleç (Middle East Technical University, Ankara) and Durmuş Boztuğ (Cumhuriyet University, Sivas) for their editorial comments and suggestions. The critical reviews from Ömer Işık Ece (İstanbul Technical University, İstanbul) and an anonymous reviewer are greatly appreciated.

References

ADAMIA, S.A., CHLEHOTVA, M.B., KEKELIA, M., LORDKIPANIDZE, M., SHAVISHILI, I. & ZACHARIAZADZE, G.S. 1981. Tectonic of the Caucaus and adjoining regions. *Journal of Structural Geology* **3**, 437–44.

AKÇAY, M. 2003. Geochemistry of the footwall- and the hanging-wall dacites of the volcanogenic massive sulphide deposits in northeastern Turkey: a new exploration tool for the Kuroko type deposits. *Syposium on the Geology and Mining Potential of Eastern Black Sea Region (Trabzon, NE Turkey)*, p. 81–83.

AKÇAY, M. 2008. Geochemistry of the footwall and the hanging-wall dacites of the volcanogenic massive sulfide deposits in northeastern Turkey: a new exploration tool for the Kuroko type deposits. *Ore Geology Reviews* [in press].

AKÇAY, M. & MOON, C.J. 2001. Geochemistry of pyrite-bearing and purple dacites in north-eastern Turkey: a new exploration tool for the Kuroko type deposits. *In:* PIESTRZYSKI, A. (ed) *Mineral Deposits at the Beginning of the 21st Century*. Krakow, Poland, p. 210–213.

AKINCI, Ö.T. 1980. Major copper metallogenetic units and genetic igneous complexes of Turkey. *In:* JANKOVIÇ, S. & SILLITOE, R. (eds), *European Copper Deposits*. Belgrade, Belgrade University, Faculty of Geology and Mining, 199–208.

ALLEN, R.L. 1988. False pyroclastic textures in altered silicic lavas, with implications for volcanic-associated mineralization. *Economic Geology* **83**, 1424–1446.

ALMODÓVAR, G.R., SAEZ, R., PONS, J.M., MAESTRE, A., TOSCANO, M. & PASCUAL, E. 1998. Geology and genesis of the Aznalcóllar massive sulphide deposits, Iberian pyrite belt, Spain. *Mineralium Deposita* **33**, 111–136.

ANGEL, B.R. & VINCENT W.E.J. 1978. Electron spin resonance studies of iron oxides associated with the surface of kaolins. *Clays and Clay Minerals* **26**, 263–272.

ANTONOVIĆ, A., GÖYMEN-ASLANER, G. & STOJANOV, R. 1996. New data on the Lahanos and Maden tepe localities, Giresun County, Eastern Black Sea Coast, Turkey. *Geologica Macedonia* **10**, 57–65.

ARRIBAS, A.J.R. 1995. Characteristics of high-sulfidation epithermal deposits, and their relation to magmatic fluid. *In*: THOMPSON, J.F.H. (ed), *Magmas, Fluids, and Ore Deposits*. Mineralogical Association of Canada, Short Course **23**, 419–454.

ARSLAN, M. & ASLAN, Z. 2006. Mineralogy, petrography and whole-rock geochemistry of the Tertiary granitic intrusions in the Eastern Pontides, Turkey. *Journal of Asian Earth Sciences* **27**, 177–193.

ARSLAN, M., BOZTUĞ, D., TEMİZEL, İ., KOLAYLI, H., ŞEN, C., ABDİOĞLU, E., RUFFET, G. & HARLAVAN, Y. 2007. $^{40}Ar/^{39}Ar$ geochronology and Sr-Pb isotopic evidence of post-collisional exensional volcanism of the Eastern Pontide paleo-arc, NE Turkey. *Geochimica Cosmochimica Acta*, Cologne, A38.

ARSLAN, M., TÜYSÜZ, N., KORKMAZ, S. & KURT, H. 1997. Geochemistry and Petrogenesis of the Eastern Pontide Volcanic Rocks, Northeast Turkey. *Chemie der Erde* **57**, 157–187.

BARRETT, T.J. 1992. Mass changes in the Galapagos hydrothermal mounds: near-axial sediment transformation and mineralization. *Geology* **20**, 1075–1078.

BARRETT, T.J., CATTALANI, S. & MACLEAN, W.H. 1993b. Volcanic lithogeochemistry and alteration at the Delbridge massive sulfide deposit, Noranda, Quebec. *Journal of Exploration Geochemistry* **48**, 135–173.

BARRETT, T.J. & MACLEAN, W.H. 1991. Chemical, mass, and oxygen-isotopic changes during extreme hydrothermal alteration of an Archean rhyolite, Noranda. *Economic Geology* **86**, 406–414.

BARRETT, T.J. & MACLEAN, W.H. 1994. Mass changes in hydrothermal alteration zones associated with VMS deposits in the Noranda area. *Exploration and Mining Geology* **3**, 131–160.

BARRETT, T.J. & MACLEAN, W.H. 1999. Volcanic sequences, lithogeochemistry, and hydrothermal alteration in some bimodal volcanic-associated massive sulfide systems. *In:* BARRIE, C.T. & HANNINGTON, M.D. (eds), *Volcanic-Associated Massive Sulfide Systems: Processes and Examples in Modern and Ancient Settings*. Reviews in Economic Geology **8**, 101–131.

BARRETT, T.J., MACLEAN W.H., CATTALANI, S. & HOY, L. 1993a. Massive sulfide deposits of the Noranda area, Quebec; V: the Corbet mine. *Canadian Journal of Earth Sciences* **30**, 1934–1954.

BARRETT, T.J., THOMPSON, J.F.H. & SHERLOCK, R.L. 1996. Stratigraphic, lithologeochemical and tectonic setting of the Kutcho Creek massive sulfide deposit, northern British Columbia. *Exploration and Mining Geology* **5**, 309–338.

BARRIGA, F.J.A.S. & FYFE, W.S. 1988. Giant pyritic base-metal deposits: the example of Feitais (Aljustrel, Portugal). *Chemical Geology* **69**, 331–343.

BEKTAŞ, O. 1987. Volcanic belts as markers of the Mesozoic–Cenozoic active margin of Eurasia-Discussion. *Tectonophysics* **141**, 345–347.

BEKTAŞ, O., ŞEN, C., ATICI, Y. & KÖPRÜBAŞI, N. 1998. Migration of the upper Cretaceous subduction-related volcanism toward the back arc basin of the eastern Pontide magmatic arc (NE Turkey). *Third International Turkish Geology Symposium, METU-Ankara, Abstracts*, p. 179.

BOZTUĞ, D., JONCKHEERE, R., WAGNER, G.A. & YEĞİNGİL, Z. 2004. Slow Senonian and fast Paleocene–early Eocene uplift of the granitoids in the Central Eastern Pontides, Turkey: Apatite fission-track results. *Tectonophysics* **382**, 213–228.

BOZTUĞ, D., ERÇİN, A.İ., KURUÇELİK, M.K., GÖÇ, D., KÖMÜR, İ. & İSKENDEROĞLU, A. 2006. Geochemical characteristics of the composite Kaçkar batholith generated in a Neo-Tethyan convergence system, Eastern Pontides, Turkey. *Journal of Asian Earth Sciences* **27**, 286–302.

BOZTUĞ, D., JONCKHEERE, R.C., WAGNER, G.A., ERÇİN, A.İ. & YEĞİNGİL, Z. 2007. Titanite and zircon fission-track dating resolves successive igneous episodes in the formation of the composite Kaçkar batholith in the Turkish Eastern Pontides. *International Journal of Earth Sciences* **96**, 875–886.

BRINDLEY, G.W. 1980. Quantitative X-ray mineral analysis of clays. *In:* BRINDLEY, G.W. & BROWN, G. (eds), *Crystal of Clay Minerals and their X-ray Identification*, 411–438.

BRYNDZIA, L.T., SCOTT, S.D. & FARR, J.E. 1983. Mineralogy, geochemistry, and mineral chemistry of siliceous ore and altered footwall rocks in the Uwamuki 2 and 4 deposits, Kosaka mine, Hokuroku district, Japan. *Economic Geology Monograph* **5**, 507–522.

ÇAĞATAY, M.N. 1993. Hydrothermal alteration associated with volcanogenic sulfide deposits; Examples from Turkey. *Economic Geology* **88**, 606–621.

ÇAĞATAY, M.N. & BÖYLE, D.R. 1977. Geochemical Prospecting for volcanogenic sulphide deposits in the eastern Black Sea ore province. *Journal of Geochemical Exploration* **8**, 49–71.

ÇAĞATAY, M.N. & EASTOE, C.J. 1995. A sulfur isotope study of volcanogenic massive sulfîde deposits of the Eastern Black Sea province, Turkey. *Mineralium Deposita* **30**, 55–66.

CALLAGHAN, T. 2001. Geology and host-rock alteration of the Henty and Mount Julia gold deposits, Western Tasmania. *Economic Geology* **96**, 1073–1088.

CUTTLER, A.H. 1981. Further studies of ferrous iron doped synthetic kaolinite dosimetry of X-ray induced effects. *Clay Minerals* **16**, 69–80.

DIXON, C.J. & PEREIRA, J. 1974. Plate tectonics and mineralization in the Tethyan region. *Mineralium Deposita* **9**, 185–198.

EĞİN, D., HIRST, D.M. & PHILIPS, R. 1979. The petrology and geochemistry of volcanic rocks from the northern Harşit River area, Pontide Volcanic Province, northeast Turkey. *Journal of Volcanology and Geothermal Research* **6**, 105–123.

FRANKLIN, J.M., LYDON, J.W. & SANGSTER, D.F. 1981. Volcanic-associated massive sulfide deposits. *Economic Geology 75th Anniversary Volume*, 485–627.

GIBSON, H.L., MORTON, R.L. & HUDAK, G.J. 1999. Submarine volcanic processes, deposits, and environments favorable for the location of volcanic-associated massive sulfide deposits. *Reviews in Economic Geology* **8**, 13–51.

GÜVEN, İ.H. 1993. *Doğu Pontidler'in 1:25.000 Ölçekli Kompilasyonu* [*1:25.000 Scale Compilation of the Eastern Pontides*]. General Directorate of Mineral Research and Exploration Institute (MTA) of Turkey [unpublished].

GÜVEN, N. 1988. Smectites. *In:* BAILEY, S.W. (ed), *Hydrous Phyllosilicates*. Mineralogical Society of America, Washington, DC. Reviews in Mineralogy **19**, 497–559.

HART, T., GIBSON, H.L. & LESHER, C.M. 2004. Trace element geochemistry and petrogenesis of felsic volcanic rocks associated with volcanogenic Cu-Zn-Pb massive sulfide deposits. *Economic Geology* **99**, 1003–1013.

HEMLEY, J.J., MONTOYA, J.W., MARINENKO, J.W. & LUCE, R.W. 1980. Equilibria in the system Al_2O_3-SiO_2-H_2O and some general implications for alteration/mineralization processes. *Economic Geology* **75**, 210–228.

HERBILLON, A.J., MESTDAGH, M.M., VIELVOYE, L. & DEROUANE, E.G. 1976. Iron in kaolinite with special reference to kaolinite from tropical soils. *Clay Minerals* **11**, 201–220.

HERRMANN, W. & HILL, A.P. 2001. The origin of chlorite-tremolite-carbonate rocks associated with the Thalanga volcanic-hosted massive sulfide deposit, north Queensland, Australia. *Economic Geology* **96**, 1149–1173.

HERMANN, W. & BERRY, R.F. 2002. MINSQ-a least squares spreadsheet method for calculating mineral proportions from whole rock major element analyses, Geochemistry. *Exploration, Environment, Analysis* **2**, 361–368.

HILL, I.G., WORDEN, R.H. & MEIGHAN, I.G. 2000. Yttrium: the immobility-mobility transition during basaltic weathering. *Geology* 28, 923 926.

HORTON, D.G. 1985. Mixed-layer illite/smectite as a paleotemperature indicator in the Amethyst vein system, Creede district, Colorado, USA. *Contribution to Mineralogy and Petrology* **91**, 171–179.

INOUE, A. 1995. Formation of clay minerals in hydrothermal environments. *In:* VELDE, B. (ed), *Origin and Mineralogy of Clays*. Springer, 268–329.

INOUE, A. & UTADA, M. 1983. Further investigations of a conversion series of dioctahedral mica/smectites in the Shinzan hydrothermal alteration area, Northeast Japan. *Clays and Clay Minerals* **31**, 401–412.

INOUE, A., VELDE, B., MEUNIER, A. & TOUCHARD, G. 1988. Mechanism of illite formation during smectite-to-illite conversion in a hydrothermal system. *American Mineralogist* **73**, 1325–1334.

ISHIKAWA, Y., SAWAGUCHI, T., IWAYA, S. & HORIUCHI, M. 1976. Delineation of prospecting targets for Kuroko deposits based on modes of volcanism of underlying dacite and alteration haloes. *Mining Geology* **26**, 105–117 [in Japan with English abstract].

JACKSON, M.L. 1956. *Soil Chemical Analysis-Advanced Course*. Published by the author, Department of Soil Science, University of Wisconsin, Madison.

KHIN, Z. & LARGE, R.R. 1992. The precious metal-rich South Hercules mineralisation, western Tasmania: a possible subsea-floor replacement volcanic-hosted massive sulphide deposit. *Economic Geology* **87**, 931–952.

KOMUSINSKI, J., STOCH, L. & DUBIEL, S.M. 1981. Application of electron paramagnetic resonance and Mössbauer spectroscopy in the investigation of kaolinite-group minerals. *Clays and Clay Minerals* **29**, 23–30.

KUNZE, G.W. 1965. Pretreatments for mineralogical analysis. *In*: BLACK, C.A. (ed), *Methods of Soil Analysis. Part I Agronomy.* American Society of Agronomy, Madison, Wisconsin, 568 577.

LARGE, R.R. 1992. Australian volcanic-hosted massive sulphide deposits: features, styles, and genetic models. *Economic Geology* **87**, 549–572.

LARGE, R.R., GEMMEL, J.B., PAULICK, H. & HUSTON, D.L. 2001. The alteration box plot: A simple approach to understanding the relationship between alteration mineralogy and lithogeochemistry associated with volcanic-hosted massive sulphide deposits. *Economic Geology* **96**, 957–971.

LEISTEL, J.M., MARCOUX, E., THIÉBLEMONT, D., QUESADA, C., SÁNCHEZ, A., ALMODÓVAR, G.R., PASCUAL, E. & SÁEZ, R. 1998. The volcanic-hosted massive sulphide deposits of the Iberian Pyrite Belt. *Mineralium Deposita* **33**, 2–30.

LEITCH, C.H.B. 1981. Mineralohy and textures of the Lahanos and Kızılkaya massive sulphide deposits, northeastern Turkey, and their similarity to Kuroko ores. *Mineralium Deposita* **16**, 241–257.

LENTZ, D.R. 1999. Petrology, geochemistry, and oxygen isotope interpretation of felsic volcanic rocks and related rocks hosting the Brunswick No. 6 and No. 12 massive sulfide deposits, Bathurst Mining Camp, New Brunswick, Canada. *Economic Geology* **94**, 57–86.

LENTZ, D.R. & GOODFELLOW, W.D. 1996. Intense silicification of footwall sedimantery rocks in the stockwork alteration zone beneath the Brunswick No. 12 massive sulphide deposit, Bathurst, New Brunswick. *Canadian Journal of Earth Sciences* **33**, 284–302.

LYDON, J.L. 1988. Volcanogenic massive sulphide deposits. Part 2: genetic models. *Geoscience Canada Reprints Series* **3**, 155–182.

MACLEAN, W.H. 1990. Mass change calculations in altered rock series. *Mineralium Deposita* **25**, 44–49.

MACLEAN, W.H. & KRANIDIOTIS, P. 1987. Immobile elements as monitors of mass transport in hydrothermal alteration: Phelps Dodge massive sulfide deposit, Matagami. *Economic Geology* **82**, 951–962.

MARUMO, K. 1989. Genesis of kaolin minerals and pyrophyllite in Kuroko deposits of Japan; implications for the origins of the hydrothermal fluids from mineralogical and stable isotope data. *Geochimica et Cosmochimica Acta* **53**, 2915–2924.

MEHRA, O.P. & JACKSON, M.L. 1960. Iron oxide removal from soils and clays by a dithionite-citrate system buffered by sodium bicarbonate. *Clays and Clay Minerals* **7**, 317–327.

MESTDAGH, M.M., VIELVOYE, L. & HERBILLON, A.J. 1980. Iron in kolinite. II. The relationship between kaolinite crystallinity and iron content. *Clay Minerals* **15**, 1–13.

NEWMAN, A.C.D. & BROWN, G. 1987. The chemical constitution of clays. *In:* NEWMAN, A.C.D. (ed), *Chemistry of Clays and Clay Minerals*. Mineralogical Society Monograph **6**, 1–128.

OHMOTO, H. 1996. Formation of volcanogenic massive sulphide deposits: the Kuroko perspective. *Ore Geology Reviews* **10**, 135–177.

OKAY, A.İ. & ŞAHİNTÜRK, Ö. 1997. Geology of the Eastern Pontides. *In:* ROBINSON, A.G. (ed), *Regional and Petroleum Geology of the Black Sea and Surrounding Region*. AAPG Memoir **68**, 291–311.

PAULICK, H., HERRMANN, W. & GEMMELL, J.B. 2001. Alteration of felsic volcanics hosting the Thalanga massive sulfide deposit (Northern Queensland, Australia) and geochemical proximity indicators to ore. *Economic Geology* **96**, 1175–1200.

PAULICK, H. & MCPHIE, J. 1999. Facies architecture of the felsic lava-dominated host sequence to the Thalanga massive sulfide deposit, Lower Ordovician, northern Queensland. *Australian Journal of Earth Sciences* **46**, 391–405.

PEARCE, J.A. 1983. Role of the sub-continental lithosphere in magma genesis at active continental margins. *In:* HAWKESWORTH, C.J. & NORRY, M.J. (eds), *Continental Basalts and Mantle Xenoliths*. Shiva, Cheshire, U.K., 230–249.

PEARCE, J.A. 1996. A user's guide to basalt discrimination diagrams. *In:* WYMAN, D.A. (ed), *Trace Element Geochemistry of Volcanic Rocks: Applications for Massive Sulphide Exploration*. Geological Association Canada, Short Course Notes **12**, 79–113.

PEJATOVIÇ, S. 1979. *Metallogeny of the Pontide-type Massive Sulphide Deposits*. Mineral Research and Exploration Institute of Turkey (MTA) Special Publications **177**, Ankara, Turkey.

PETER, J.M. & GOODFELLOW, W.D. 1996. Mineralogy, bulk and rare earth element geochemistry of massive sulphide-associated hydrothermal sediments of the Brunswick Horizon, Bathurst Mining Camp, New Brunswick. *Canadian Journal of Earth Sciences* **33**, 252–283.

RAGLAND, P.C. 1989. *Basic Analytical Petrology*. Oxford University Press, Oxford, UK.

RENGASAMY, R. 1976. Substitution of iron and titanium in kaolinites. *Clays and Clay Minerals* **24**, 264–266.

SÁNCHEZ-ESPAÑA, J., VELASCO, F. & YUTSA, I. 2000. Hydrothermal alteration of felsic volcanic rocks associated with massive sulphide deposition in the Northern Iberian Pyrite Belt (NW Spain). *Applied Geochemistry* **15**, 1265–1290.

SANGSTER, D.F. 1972. *Precambrian Volcanogenic Massive Sulfide Deposits in Canada: A Review*. Geological Survey of Canada Paper 72–22.

SANTAGUIDA, F., HANNINGTON, M.D. & JOWETT, E.C. 1992. An alteration and sulphur isotope study of the Pilley's Island massive sulphides, Central Newfoundland *In*: *Current Research, Part A. Geological Survey of Canada Paper* **92-1D**, 265–274.

SATO, T. 1977. Kuroko deposits: their geology, geochemistry and origine. *In*: *Volcanic Processes in Ore Genesis*. Geological Society, of London, Special Publications **7**, 153–161.

SCHARDT, C., COOKE, D.R., GEMMELL, J.B. & LARGE, R.R. 2001. Geochemical modeling of the zoned footwall alteration pipe, Hellyer volcanic-hosted massive sulfide deposits, western Tasmania, Australia. *Economic Geology* **96**, 1037–1054.

SCHNEIDER, H.J., ÖZGÜR N. & PALACIOS, C.M. 1988. Relationship between alteration, rare earth element distribution and mineralisation of the Murgul copper deposit, northern Turkey. *Economic Geology* **83**, 1238–1246.

ŞENGÖR, A.M.C. & YILMAZ, Y. 1981. Tethyan evolution of Turkey: A plate tectonic approach. *Tectonophysics* **75**, 181–241.

SHARPE, R. & GEMMELL, J.B. 2001. Alteration characteristics of the Archean Golden Grove Formation at the Gossan Hill deposit, Western Australia: Induration as a focussing mechanism for mineralizing hydrothermal fluids. *Economic Geology* **96**, 1239–1262

SHIKAZONO, N. 2003. *Geochemical and Tectonic Evolution of Arc-backarc Hydrothermal Systems: Implications for the Origin of Kuroko and Epithermal Vein-type Mineralizations and the Global Geochemical Cycle*. Elseiver, Amsterdam.

SHRIVER, N.A. & MACLEAN, W.H. 1993. Mass, volume and chemical changes in the alteration zone at the Norbec mine, Noranda, Quebec. *Mineralium Deposita* **28**, 157–166.

SILLITOE, R.H. 1993. Epithermal models: genetic types, geometrical controls and shallow features. *In:* KIRKHAM, R.V., SINCLAIR, W.D., THORPE, R.I. & DUKE, J.M. (eds), *Mineral Deposit Modeling*. Geological Association of Canada, Special Paper **40**, 403–417.

SIMMONS, S.F. & BROWNE, P.R.L. 1990. Mineralogic, alteration and fluid inclusion studies of epithermal gold-bearing veins at the Mt. Muro prospect, Central Kalimantan (Borneo), Indonesia. *Journal of Geochemical Exploration* **35**, 63–104.

ŚRODOŃ, J. & EBERL, D.D. 1984. Illite. *In:* BAILEY, S.W. (ed), *Micas.* Mineralogical Society of America, Reviews in Mineralogy **13**, 495–544.

STEINER, A. 1968. Clay minerals in hydrothermally altered rocks at Wairakei, New Zealand. *Clays and Clay Minerals* **18**, 165–177.

SUN, S. & MCDONOUGH, W.F. 1989. Chemical and isotopic systematics of oceanic basalt. *In:* SAUNDERS, A.D. & NORRY, M.J. (eds), *Implications for Mantle Composition and Processes, Magmatism in the Ocean Basins*. Geological Society, London, Special Publications **42**, 313–345.

TAYLOR, S.R. & MCLENNAN, S.M. 1985. *The Continental Crust, Its Composition and Evolution*. Blackwell, Oxford.

TOKEL, S. 1972. *Stratigraphical and Volcanic History of the Gümüşhane Region, NE Turkey*. PhD Thesis, University College London, UK [unpublished]

TOKEL, S. 1977. Eocene calc-alkaline andesites and geotectonism in the Eastern Black Sea region. *Bulletin of the Geological Society of Turkey* **20**, 49–54 [in Turkish with English abstract].

TOPUZ, G. 2002. Retrograde P–T path of anatectic migmatites from the Pulur Massif, Eastern Pontides, NE Turkey: petrological and microtextural constraints. *First International Symposium of the Faculty of Mines (İTÜ) on Earth Sciences and Engineering Abstracts*, İstanbul, Turkey, p. 110.

TOPUZ, G., ALTHERR, R., SATIR, M. & SCHWARZ, W. 2001. Age and metamorphic conditions of low-grade metamorphism in the Pulur Massif, NE Turkey. *Fourth International Turkish Geology Symposium Abstracts, Adana, Turkey*, p. 215.

TÜYSÜZ, N. 2000. Geology, Lithogeochemistry and genesis of the Murgul massive sulfide deposit, NE-Turkey. *Chemie der Erde* **60**, 231–250.

URABE, T. & MARUMO, K. 1991. A new model for Kuroko-type deposits of Japan. *Episodis* **14**, 246–251.

URABE, T., SCOTT, S.D. & HATTORI, K. 1983. A comparison of footwall-rock alteration and geothermal systems beneath some Japanese and Canadian volcanogenic massive sulphide deposits. *Economic Geology Monograph* **5**, 345–364.

UTADA, M. & ISHIKAWA, T. 1973. Alteration zones surrounding "Kuroko-type" ore deposits in Nishiaizu District-especially the analcime zone for an indicator of exploration of the ore deposits: *Mining Geology of Japan* **23**, 213–226 [in Japanese with English abstract].

WEAVER, C.E. & POLLARD, L.D. 1973. *The Chemistry of Clay Minerals*. Developments in Sedimentology **15**, Elsevier Scientific Publication Amsterdam.

WINCHESTER, J.A. & FLOYD, P.A. 1977. Geochemical discrimination of different magma series and their differentiation producst using immobile elements. *Chemical Geology* **20**, 325–343.

YILDIZ, Ş. 1988. *Geology, Reserv and Leaching Properties of the Kutlular (Sürmene) Massive Sulphide Deposit*. MSc Thesis, Karadeniz Technical University, Trabzon, Turkey [in Turkish with English abstract, unpublished].

YILMAZ, Y. 1972. *Petrology and Structure of the Gümüşhane Granite and Surrounding Rocks, North-Eastern Anatolia.* PhD Thesis, University of London [unpublished].